IGM88RT-401-721-G
CNRC 28901

ULTRASONIC MONITORING OF FLOAT ZONE IN GERMANIUM RODS

C.K. Jen and J.F. Bussiere

Industrial Materials Research Institute
National Research Council of Canada
75 Boul. de Mortagne, Boucherville,
Quebec, Canada J4B 6Y4

and

Ph. de Heering

Canadian Astronautics Ltd.
105 Morrison Drive,
Ottawa, Ontario K2H 8K7

ABSTRACT

The growth of high-purity Germanium single crystals is described for the fabrication of sensitive high resolution gamma ray detectors. Such crystals are normally obtained by the standard Czochralski method and then purified by the float zone technique. Under normal gravity conditions, the maximum processable size is limited by the float zone process and a program has been initiated to produce large crystals under microgravity conditions. As part of this program, ultrasonic techniques have been investigated for the real-time monitoring of the molten Ge zone and will be reported in this report.

The propagation of acoustic waves in anisotropic single crystal rods of Ge have been investigated. In particular, effects of diffraction and mode conversion on received echoes of longitudinal and shear waves are described. Experimental measurements obtained during zone refining of small diameter Ge rods using water-cooled shear and longitudinal transducers at each end are then presented. It is shown that arrival times and amplitudes of the reflected signals from the solid-liquid Ge interface can be used for monitoring purposes and that good resolution can be obtained for both zone position and thickness. Acoustic energy transfer at the solid-liquid interface, observed even in the case of shear waves, is discussed in terms of mutiple mode conversion. Preliminary experimental tests with transducers operating at high temperature are also presented.

1. INTRODUCTION

Solid-state Germanium (Ge) single crystals are an essential part of gamma ray detectors. The detector sensitivity is proportional to the purity and the size of the Ge crystal. The high purity is normally achieved by using the standard czochralski crystal growth method to obtain the desired size and then the float zone refining technique to enhance the purity. It is known that the size of the Ge crystal for the float zone method is limited on earth due to gravity. Therefore it has been proposed that float zone refining to be performed in space in order to obtain the very high purity for the desired crystal size.

The float zone method is currently applied to Ge single crystals with a cylindrical rod geometry at Cominco Ltd (Trail, B.C.) who is also an industrial collaborator for this project. The float zone consists of a narrow section of molten (liquid) Ge and the melting temperature for germanium is 936°C. The heat is supplied by a high power radio frequency (RF) source through the conducting coils which encircle but do not contact the Ge rod. In order to have a uniform purity across the radial direction of the Ge rod the molten zone has to extend from the periphery to the center of the rod. It also seems that the narrower the thickness of the melt the better is the quality of the crystal. Naturally, minimum heating is desirable for any experiment performed in space or on earth. Therefore a monitor for this float zone may be desired. The purpose of the monitor is (i) to detect whether the melt is complete, (ii) to know the location of the melt with high ranging resolution and (iii) to obtain more information on the melt such as the shape of the interface between the solid and liquid Ge and the thickness of the melt.

Because of the melt the temperature at the end of the Ge rod is found to be approximately 500°C under the present experimental considerations determined by Canadian Astronautics Ltd. At such high temperature there are two potential methods to perform the proposed ultrasonic measurement. One is to use an ultrasonic transducer bonded to a water cooled buffer rod which is a section of the Ge rod, and another is to find an ultrasonic transducer and a coupling material capable of operation at 500°C. It is obvious that the experiments performed in space should pay much attention to the weight constraint induced by cost considerations. Because of this concern the former method is not very economical. However, the latter method will demand transducers and coupling materials which are not currently available commercially.

In this report, Section II addresses the acoustic wave propagation properties in the anisotropic Ge rods. In Section III the acoustic properties of Ge at elevated temperatures as well as priliminary tests on some potentially usable transducers and coupling materials are given. Section IV demonstrates the feasibilty of the ultrasonic method for monitoring the float zone. Concerns related to crystal growth under an ultrasonic field are discussed in Section V. Section VI concludes this study

and future directions are outlined.

II. ACOUSTIC WAVE PROPAGATION IN GERMANIUM RODS

Single crystal Ge has the cubic symmetry along its principal axis which is also the axis of the Ge rod for this project. Although the propagation of acoustic waves in rods has been studied previously for the isotropic [1-4] and anisotropic [5-7] cases, there seems a lack of analysis for rods with diameters between a few and tens of acoustic wavelengths. At present, the Ge samples used in the float zone project are of such size. Furthermore, the diameter of Ge rods to be refined in space may be practically larger than 6 cm which is more than 50 acoustic wavelengths intended for the experiments. Therefore theoretical investigations are focused on the bulk planar acoustic propagation properties of Ge single crystals in this section. In the experiments isotropic aluminum (Al) and anisotropic Ge rods are used as samples. The experimental results for rod samples are then compared with theoretical predictions.

II.1 Theory

In an isotropic, homogeneous and lossless 'bulk' material longitudial and shear plane waves will propagate along their wave vector $\vec{k}$ with no disturbance coming from the boundary. The Poynting vector $\vec{p}$ (the energy flow direction) always points in the same direction as $\vec{k}$ and wave diffraction also exists. Diffraction causes the width of collimated waves to increase after travelling a certain distance.

Figure 1 shows some typical slowness curves for isotropic and anisotropic materials (1/v, where v is the acoustic velocity). Since $|\vec{k}| = 2\pi/\lambda = 2\pi f/v$, the slowness curves are identical to wavenumber $\vec{k}$ curves under a same operating frequency f [8,9]. The direction of Poynting vector $\vec{p}$ is always perpendicular to the tangential plane (here, only lines are shown) drawn where $\vec{k}$ intersects the slowness plane (here, only curves are shown). Curve A in figure 1 is an isotropic case. For the isotropic case the direction of $\vec{p}$ is the same as that of $\vec{k}$. In anisotropic crystals indicated as curves B, C and D, the direction of $\vec{p}$ is very often different with that of $\vec{k}$. Analogous to ray optics the plane acoustic waves expressed by acoustic rays can exhibit diverging (curve B), collimating (C) and focusing (curve D) phenomena, thus their diffraction loss may be larger or smaller than that of the isotropic case [10-14].

In any direction of a bulk medium there always exists one quasi (or pure) longitudinal and two quasi (or pure) shear waves and the particle displacements of these three waves are orthogonal to each other [8]. Figure 2 shows the slowness curves of an isotropic Al. Both longitudinal (curve L) and shear waves (curves S1 & S2) are pure modes. In any isotropic material two shear waves are degenerated and thus have the same velocity. They are

plotted as one single trace in Fig.2.

The slowness curves of Ge crystal in the <100> [001] plane is given in Figure 3 and because of the cubic symmetry those in the <100> [010] and <010> [001] planes are identical. It is noted that all the slowness curves in the report are calculated from the computer program developed in Ref.[14], and < > and [ ] represent the direction of the horizontal (east) and vertical (north) axis respectively in each figure. In Figure 3 along the crystal axis (<100> or <010> or <001>), one shear wave (S1) is isotropic, and the longitudinal (L) and another shear (S2) exhibit higher diverging and focusing than the isotropic case respectively. The numerical values of the inverse of the phase velocity (vpinv) , phase velocity (vp), power flow angle (angp) and particle displacement orientations (uX, uY, uZ) for three waves (one pure longitudinal, two pure shear) along the <100> propagation direction are given in Table 1. The detailed explanation of these designations can be found in Ref.[15]. It is noted that each shear wave is polarized parallel to one of the crystalline axes in the transverse plane.

Table 1 The Acoustic Wave Properties Along <100> direction

		longitudinal	shear 1	shear 2
vp (m/s)		4924.2	3548.8	3548.8
vpinv (s/m)		.0002031	.0002818	.0002818
angp		0	0	0
u	X,<100>	1.0	0	0
	Y,<010>	0	0	1.0
	Z,<001>	0	1.0	0

For comparison, the slowness curves of Ge in the <11-2> [111], <-110> [111] and <11-2> [-110] planes are shown in Figures 4(a)-(c) respectively. It is noted that since the direction of p is normal to the tangential plane at the intersection of k and the slowness curve of a particular mode, in general a three dimensional display is required. For simplicity, only three orthogonal planes are shown here. Both <11-2> [111] and <-110> [111] planes contain <111> axis, and <11-2> [110] plane is perpendicular to the <111> axis. Along the <111> direction the longitudinal wave (curve 1) exhibits very good collimating property but shear modes (curves 2&3) diverge very much.

In Refs.[10-14] it has been reported that for longitudinal acoustic waves a parameter b may be used to estimate the acoustic anisotropy which causes the anomalous diffraction. This b may be

defined as follows [10-14]: If the slowness curve in the vicinity of a symmetry axis is adequately approximated by a power series

$$k(\theta) = k_0 (1 + b\theta^2 + d\theta^4 + ...) \qquad (1)$$

and terms higher than quadratic are neglected. When $\vec{k}$ deviates from the symmetry axis ($k = k_0$) by O, then the power flow angle will deviate by $(1 - 2b)\theta$. It should be mentioned that Eqn.(1) can only deduce a value of b in a 2-D representation (slowness curve), a more proper value should be obtained with a 3-D representation (slowness surface). This means that an averaged value of b obtained from many slowness curves should be adopted.

In general, a large negative b means that the beams suffer more diffraction loss and a positive b implies less. b is equal to zero for an isotropic material [11-13]. It can be also said that the collimation of acoustic beams in anisotropic modes is proportional to the (1-2b) [13,14]. Here Ge having a cubic crystal symmetry is used as an example to compare the analytic expressions given in [11] and the graphic representations in this report.

Along <100> direction

$$b = \frac{(C_{11} - C_{12} - 2C_{44})(C_{11} + C_{12})}{2C_{11}(C_{11} - C_{44})} = -0.58$$

and along <111> direction of a cubic system

$$b = \frac{2(C_{44} + C_{12} - C_{11})(C_{11} + 2C_{12} + C_{44})}{3(C_{12} + C_{44})(C_{11} + 2C_{12} + 4C_{44})} = 0.18$$

Along <100> direction of Ge (see Fig.3) the longitudinal waves exhibit a little more diverging than the isotropic case and along <111> direction they show some collimating effect (see Fig.4), thus b is a negative and a positive number for the former and the latter case respectively. The graphic estimations of the degree of anisotropy have been also checked for many materials especially those listed in Table I in Ref.[12] and very good agreement has been obtained. Since the analysis to date on the diffraction of acoustic waves has been limited to a three, four, or sixfold pure mode axis [10-13], the graphic representation by slowness curves, which not only may deduce the parameter b [14] but also gives more general information on the beam collimation, is adopted here.

When the diameter of a rod is around 10 mm, which is equivalent to a few or tens of acoustic wavelengths for the operating frequencies chosen for the experiments, the cylindrical boundary will disturb the plane acoustic waves and alter the propagation properties. If along the rod axis an acoustic mode exhibits

focusing, collimating or diverging effect, then the boundary will contribute less or more disturbance. It is again noted that the current experimental setup uses Ge rods of a diameter around 10 mm, however it is expected that the final size of the rod diameter for the zone refining process in space may be more than 6 cm.

II.2 Experiment

Since both longitudinal and shear types of waves may be used, they are discussed seperately. In general, longitudinal waves are easier for excitation and detection, and convenient for operation at room or elevated temperatures, in particular concerning the coupling materials between the transducer and the Ge rod. However, shear waves are expected to have a larger reflection coefficient at the solid-liquid interface.

In the experiments a wideband system which consists of a MP203 pulser and a MR101 receiver from Metrotek (Richland, WA) was used. The ultrasonic transducers were broadband (damped) types and from Ultran (State College, Penn) or Panametrics (Waltham, Mass). The reasons for the selection of broadband transducers are (i) the ultrasonic attenuation in Ge single crystal is very small [16]. For instance, at 100 MHz the attenuation for longitudinal and shear waves is only about 0.4 and 0.2 db/cm respectively; (ii) the damped transducer provides better range resolution and (iii) the frequency spectrum of the acoustic signals may give more information on the float zone. However, it is noted that highly damped transducers have less efficiency than the lesser damped transducers.

II.2a Longitudinal Waves

Figures 5-8 (a)&(b) show the ultrasonic echoes reflected at the back surface of a Ge rod with a 10 mm diameter and 91.0 (Figs.5-7) or 340 mm (Fig.8) length using 5 MHz (12.7 mm dia), 5 MHz (6.35 mm dia.) and 15 MHz (4.57 mm dia. Figs.7&8) Ultran longitudinal transducers respectively; and in each figure (b) is a zoomed picture of (a). The rod axis is along <100> direction. For example, in Figs. 5-7 the measured time delay for the first arrived longitudinal echo is 36.7 us. It corresponds to a velocity of 4959 m/s which is less than 1% higher than the bulk longitudinal velocity along <100> direction of Ge (see Table 1). From Figs.5-8 the following three observations have been noted:

1. A few echoes arrive later than the first longitudinal echo. Some of them seem to be periodical.

2. The length of the rod does not change the time delay pattern among the echoes in 1.

3. The ratio of the amplitudes of these late arrived echoes over that of the first longitudinal echo decreases if the acoustic

operating frequency increases.

These three phenomena are certainly related to the wave diffraction inside the rod. In order to understand better about these trailing echoes, inexpensive isotropic aluminum (Al) rods of similar diameters and lengths are used. The detailed analysis is given in Appendix A. These trailing echoes have been observed in Refs.[17,18] but no detailed explanation has been given. After our investigation it is concluded that the late arrived echoes come from mode conversion processes. The longitudinal waves travelling nearly parallel to the rod axis strike rod-air boundaries with a small angle of inclination, a part of their energy is converted to shear waves which propagate across the diameter of the Al rod with an angle dictated by the phase matching requirements (see Appendix A). The phase matching demands that the wavenumber components along the interface should be equal [8,9] for each wave involved in the mode conversion. The cause of the mode conversion are mainly due to the above mentioned slight inclination of the longitudinal waves striking the rod-air boundary and minorly due to the roughness of the boundary. The measured time delays agree excellently with those predicted by the theory.

Since Ge is an acoustically anisotropic material, the wave propagation inside a Ge rod is very complicated. However, td is caused by the mode conversion process explained in Appendix A. Figures 9 and 10 show the slowness curves of Ge <100> [001] and <100> [011] plane. The mode conversion induces two shear waves which have different velocities and propagation directions. This is very different from the isotropic case explained in Appendix A. In Fig.9 the longitudinal wave L may convert to S2 (vs = 2827 m/s, $\theta = 36^{\circ}$) and S1 (vs = 3548 m/s, $\theta = 46^{\circ}$), while in Fig.10 L may convert to S2' (vs = 3036 m/s, $\theta = 36^{\circ}$) and S1' (vs = 3078 m/s, $\theta = 38^{\circ}$). Since the cylindrical rod is the actual geometry, many slowness curves including <100> direction should be studied. However, Ge has a cubic symmetry, the above mentioned two slowness curves approximately represent the two extreme cases. Since the range of acoustic velocities and mode conversion angles O's varies a great deal for S1 shear waves, the waves will not be added in phase due to lack of cylindrical symmetry. Therefore it is believed that shear waves S2 are responsible for the periodical trailing echoes. Therefore the td (time delay between echoes 'a' and 'b' in Figs.5-8) can be expressed as (see Appendix A)

$$t_d = \frac{d/\cos\theta}{vs2} - \frac{d*\tan\theta}{vl} \qquad (1)$$

where d is the diameter of the rod. Since for the S2 shear waves θ's are near 36 degrees, hence the averaged vs equal to 2931 m/s is used for the Eqn.(1). The calculated td is 2.74 us which agrees very well with the observed value of 2.8 us which is measured between the centers of the echoes 'a' and 'b'. In addition, as mentioned in Appendix A since the echo 'b' is the

source of echo 'c', the amplitude of echo 'b' must be larger than that of echo 'c'. This is verified also in Figs.5-8. Although good agreements using the mode conversion argument have been obtained between the calculated and the observed value of td for the periodical trailing echoes, no effort has been made to explain the extra echoes which appear in Figs.5-8.

It is interesting to note that along the <111> direction of Ge there exists the collimating behavior, therefore the amplitudes of the trailing echoes appearing in the <100> direction of Ge rod and isotropic Al rod (see Appendix A) are much smaller. Figures 11 (a)&(b) are the received signals from the end of a 156 mm long and 14 mm diameter Ge rod whose rod axis is the <111> orientation using a 15 MHz 4.57 mm diameter Ultran transducer in the reflection geometry. Using a 5 MHz 12.7 mm diameter Ultran transducer trailing echoes also appear but are small. Very good agreement has also been obtained between the calculated td using Eqn.(1) and the measured value.

II.2b Shear Waves

Since the available high frequency shear wave transducers at IMRI are only 5 and 2.25 MHz Panametrics transducers with a 12.7 mm diameter, all the measurements have been performed with these two types. Figures 12 and 13 (a)&(b) show the reflected signal from the end of a 10 mm diameter, 91 mm long Ge rod with the rod axis oriented in <100> direction using a 2.25 and 5 MHz transducer respectively. The measurements with a 350 mm long Ge rod will be given in Section IV. Because the shear wave has the polarization preference, the transducer can excite either stronger S1 or S2 waves shown in Fig.3. But since these two shear waves are degenerate along the <100> direction, no obvious time delay difference for the first shear echo arrival has been observed when the transducer orientation is rotated. However there are minor changes in the received amplitude. It is noted that along <100> direction, shear wave S1 is an isotropic case in the <100> [010] or <100> [001] plane, and shows slight collimation in the <100> [011] plane; however S2 shows the beam focusing effect in the above three planes [14]. If the polarization of the shear wave transducer is aligned along that of pure S2 shear wave, the received signal is stronger.

After careful examination of the phase matching conditions and the slowness curves it is concluded that for shear wave propagation there should not have the trailing echoes as appearing in the longitudinal wave measurements. Because the wavenumber component along the propagation of the shear waves is not equal to that of the longitudinal waves of any propagation direction. It means that there is no mode conversion process as observed in the longitudinal wave measurements. It has been confirmed by the results shown in Figs.12 and 13 and also figures appeared later in Section IV.

It is interesting to note that the power flow angles (ie. large

negative b) for the two shear waves of the Ge rod oriented in the <111> direction are very large, therefore it is expected that the first shear wave echo looks messier than that oriented in the <100> direction. Figure 14 is the transmitted shear wave arrivals for a 14 mm diameter 101 mm long Ge rod oriented in the <111> direction and it agrees well with the theoretical prediction.

III. CONSIDERATIONS FOR HIGH TEMPERATURE OPERATIONS

As mentioned earlier the float zone detection is also intended to be performed in space. Because of the potential limitation on the weight and power consumption, the ultrasonic transducers may be required to be operated at around 500 C Because no such transducers are currently available in the market, a preliminary study is being performed at IMRI. The considerations for high temperature operations can be categorized to transducers, coupling materials and Ge samples. They are described as follows:

III.1 Transducers

There are three piezoelectric materials commonly used as ultrasonic transducers because of their high electro-mechanical coupling (EMC) constants [21]. The limit of high temperature operation comes from their Curie temperature listed in Table 2. It is clear that only lithium niobate LiNbO3 can be used. For lithium niobate it is well known that Z cut and 36° rotated Y cut are used for longitudinal wave transducers, and X cut and 163° rotated Y cut are for shear wave transducers. Since 36° rotated Y cut and X cut have higher EMC, they are used as longitudinal and shear wave transducers and were tested at the elevated temperatures.

Table 2 Curie Temperature Of Three Piezoelectrical Materials

Material	Temp. (°C)
$LiNbO_3$	1210
Quartz	576
PZT	300

The high temperature test of the thin disc LiNbO3 transducer was performed using a setup shown in Fig.15. A copper rod is heated inside a furnace. The transducer is attached to the one end of the copper rod and a thermocouple is used to monitor the temperature. The attachment of the transducer is carried out by a connector of spring loaded contact type (Robinson Nugent, model N-120-1) shown in Fig.16 consisting of two electrical probes (positive and negative) and two springs. The spring pushes the probe to contact the gold electrode of the ultrasonic transducer,

and thus pushed the transducer to the end of the heated copper rod. The spring loaded probes were spot-welded to a BNC connector in order to be used at 500°C.

Since the LiNbO3 thin disc transducers purchased from Valpey Fisher (Hopkinton, MA) resonate at their foundamental frequency and also the harmonics. A HP 8754A Network Analyzer is used to observe these resonances by monitoring the reflected electrical signal at different frquency ranges. The constant amplitude electrical signal generator of the Network Analyzer sweeps its frequency over a frequency range, at the resonant frequency it loses part of its energy to the transducer, therefore a decrease appears in the reflection coefficient measurement. If there is a change in the transducer, the reflection coefficient will change. This is the criterion for monitoring the LiNbO3 performance at elevated temperatures.

The electrical signals of the Network Analyzer are connected to the two gold electrodes of the LiNbO3 tranducer through the spring loaded connectors. Figures 17(a),(b)&(c) were observed signals at 25, 419 and 502°C respectively. There is little change between (a) and (b) even after 24 hours. After many repeated experiments it has been also found out that the change at 502° C is due to the softening process of the thin gold electrode (2000 A° thick) not the LiNbO3. Once the temperature is cooled back to the 25°C, the signal came back as that in (a). Therefore it was concluded that LiNbO3 is good for the operation at 500° C. Since the gold film is softened at such temperatures, metallic thin films having higher melting temperatures as well as conductivity such as chromium and titanium are being considered as electrode material for the ultrasonic transducers. More dicussions about these metallic films are given below.

III.2 Coupling Materials Between The Transducer and The Ge Rod

The selection of the coupling materials can be regarded as the most challenging task in this project for high temperature operation. The material is preferred to have good mechanical bonding strength over the operated temperature range, compatible thermal expansion coefficient to the transducer and Ge rod, low acoustic attenuation, good acoustic impedance matching between the transducer and the Ge rod. Since the amplitude of the received signal will be used as one of the montoring criteria, to maintain the constant amplitude of the acoustic signal transmitted through the coupling material is also very important.

Many materials have been tested, but only the results of one hopeful ceramic cement Cotronics 989 (From Cotronics, Brooklyn, N.Y.) are presented here. This ceramic cement may be cured at room temperature for about 48 hours or at 50°C for about 12 hours. In our case the former one was often used, however there is no major difference between the two approaches. The adhesion of this particular coupling material was tested using a sandwich geometry in which Cotronics 989 was cured in between a glass

plate and one end of a Ge rod. After the curing process when we tried to seperate the glass and the Ge rod, parts of Ge rod came out with the cement. It means that there is a very strong mechanical bonding between the cement and the Ge rod.

The experimental setup for the ultrasonic test of the cement is given in Fig.18. A short Ge rod sample is put on the top of a hot plate. In the reflection geometry one LiNbO3 transducer is bonded to one end of the rod through Cotronics 989 ceramic cement. Two transducers are required in the transmission geometry. The hot plate available can only heat the Ge rod to about 350° C, therefore all the tests for coupling materials are performed within this temperature range. Again the electrical connection is achieved through the spring loaded connector connected to the proper pulser and receiver. The echoes are then monitored from the CRT of an oscilloscope.

Figures 19(a),(b)&(c) show the transmitted longitudinal signals through a 10 mm diameter 27 mm long Ge rod using a pair of 5 MHz longitudinal disc LiNbO3 transducer with a 6.35 mm diameter at 25, 200 and 350°C respectively. The reflected shear wave signals through a 10 mm 20 mm long Ge rod using a 5 MHz shear wave transducer with a 6.35 mm diameter at 25, 200, and 350°C are given in Figures 20 (a),(b)&(c) respectively. From Figures 19 and 20 we conclude that Cotronics may be used as the ultrasonic coupling material between Ge rod and the transducer. However during the cooling process, for instance from 350 to 25°C the signals did not come back as expected from (c) to (a). After the careful examination, it was found out that the adhesion between the gold electrodes normally used for the ultrasonic transducers and the Cotronics 989 is very poor. During heating the cement and the gold are in good contact because of the thermal expansion, but this does not work during cooling. Therefore an alternative electrode must be found to replace the gold electrode.

It should be noted that since the transducers used in Figs.19 and 20 did not have the backing materials which are normally used for the purpose of mechanical damping, the echo width of the received signals is much wider than those obtained with commercially available damped tranducers. At 500°C it is also very difficult to find a proper backing material. The wider width of the echo may give less range resolution.

Table 3 lists the melting temperatures and electrical resistivities of several metals with higher melting temperatures than 500°C. Mechanical bonding tests of all these materials using the above mentioned sandwich structure have been performed. It was concluded that chromium or titanium thin metal film may be used as electrodes for the ultrasonic transducers used in this project. They have high melting temperature, good conductivity, and strong bond to the Cotronics 989. At the present time many experiments related to this concern have been planned but not yet performed.

Table 3 Melting Temperatures and Electrical Resistivities Of Several Metals

Metal	Melting Temp (^{o}C)	Electrical Resistivity (microohm-cm)
Gold	1063	2.1
Chromium	1875	12.9
Titanium	1668	47.8
Platinum	1769	9.8
Aluminum	660	2.6
Nickel	1453	6.8
Silver	960	108.4

III.3 Germanium Properties

The acoustic properties of Ge at elevated temperatures have been reported in Refs.[22-26], however, only the data in Refs.[23,24] are used for the solid Ge and that in Ref.[26] for the liquid Ge here. They are listed in the Table 4. In this table the density of the solid Ge beyond 573^{o}K is extrapolated.

From Table 4 the following observations have been noted.

1. Both longitudinal and shear wave velocities and the density decrease as the temperature increases.

2. The longitudinal velocity of the liquid Ge is lower than both the longitudinal and shear wave velocities of the solid Ge, but its density is higher.

3. The wave diffraction properties of the solid Ge along <100> direction does not change significantly in the temperature range listed.

4. The ratio of the longitudinal and shear acoustic impedances of the solid Ge just below the melting temperature over the longitudinal acoustic impedance of the liquid Ge is about 1.6 and 1.2 respectively.

TABLE 4 Acoustic Properties of Ge at Elevated Temperature

TEMP (K)	DENSITY (Kg/m)	C11 (*E-11)	C12 (*E-11)	C44 (*E-11)	VL (m/s)	VS (m/s)
73.00	5339.00	1.3150	0.4948	0.6840	4962.87	3579.30
123.00	5336.00	1.3115	0.4922	0.6819	4957.65	3574.81
173.00	5331.00	1.3050	0.4900	0.6788	4947.67	3568.34
223.00	5328.00	1.2990	0.4871	0.6756	4937.67	3560.92
273.00	5324.00	1.2920	0.4845	0.6725	4926.20	3554.08
298.00	5323.00	1.2890	0.4830	0.6710	4920.94	3550.45
323.00	5321.00	1.2850	0.4819	0.6690	4914.22	3545.82
373.00	5315.00	1.2780	0.4797	0.6655	4903.59	3538.53
423.00	5312.00	1.2720	0.4776	0.6620	4893.44	3530.21
473.00	5307.00	1.2650	0.4756	0.6580	4882.26	3521.18
523.00	5302.00	1.2575	0.4738	0.6540	4870.06	3512.12
573.00	5297.00	1.2510	0.4721	0.6509	4859.75	3505.44
298.00	5323.00	1.2400	0.4130	0.6830	4826.50	3582.05
373.00	5315.00	1.2340	0.4190	0.6770	4818.43	3568.97
473.00	5307.00	1.2190	0.4160	0.6680	4792.67	3547.84
573.00	5297.00	1.2010	0.4090	0.6590	4761.64	3527.18
673.00	5287.00	1.1830	0.4010	0.6500	4730.29	3506.32
773.00	5277.00	1.1650	0.3930	0.6410	4698.61	3485.26
873.00	5267.00	1.1440	0.3840	0.6310	4660.49	3461.25
973.00	5257.00	1.1210	0.3730	0.6210	4617.79	3436.98
1073.00	5247.00	1.1000	0.3660	0.6090	4578.69	3406.85
1123.00	5242.00	1.0910	0.3650	0.6020	4562.09	3388.83
1155.00	5240.00	1.0860	0.3650	0.5960	4552.49	3372.54
1209.00	5235.00	1.0740	0.3650	0.5880	4529.43	3351.43
LIQUID	5510.00				2710.00	

IV. ULTRAOSONIC MONITORING OF THE FLOAT ZONE

As mentioned earlier the three prime objectives of the proposed ultrasonic method are to be able to (i) monitor whether the melt is complete, (ii) locate the melt with high ranging resolution and (iii) know more about the melt such as its thickness. In order to verify the feasibility, ultrasonic experiments have been carried out by Mr. Ph. de Heering of CAL at Cominco Ltd (Trail, B.C.). Each of the two ultrasonic transducers was bonded to the Ge rod end water-cooled to room temperature through the coupling material. Ultra-Gel and SWC from Panametrics were used as the coupling material for longitudinal and shear waves respectively. In the measurements both the transmitted and reflected signals are recorded. The details are described in the Ref.[27]. The primary goal of the experiments performed with the water-cooled setup is to see the reflected signal conditions from the solid-liquid Ge interface.

Figure 21 shows the reflected signals obtained using a 5 MHz shear wave transducer on a 10 mm diameter 350 mm long Ge rod oriented in the <100> direction. The measurement was recorded every one, two or four minutes and time is marked in at the righthand side of each trace. Each measurement is shown as one trace in the figure. The rod was cold (room temperature) at the lowest trace, then heated up nearly at the one third of the Ge rod by a RF heater. The heater was continuously moving toward the transducer (upward in Fig.21) at a speed about 50 mm per hour. The early arrived dominant echo is from the solid-liquid Ge interface and the last large echo is from the end of the rod. In this section two important observations are analyzed.

The first one is the time delay information. The time delay of the received signal from the end of the Ge rod increases during heating (compare the second last trace with the last trace) and decreases during cooling (second trace compared with the first trace). Furthermore, during the formation of the float zone the time delay is further decreased (see the lower traces in Fig.21) and vice versa (see the upper traces). This observation can be explained by the data listed in Table 4, where the shear wave velocity decreases as the temperature increases. In addition the longitudinal velocity of the liquid Ge is slower than that of the solid Ge just before the melting temperature.

The second observation is that the reflected shear wave signals from the end of the Ge rod are observed even with a round trip through a section of the liquid Ge (float zone). In addition the reflected signal from the solid-liquid Ge interface is strong. In general if an ideal shear wave (only having the transverse particle displacements) strikes at a solid-liquid boundary with normal incidence, all its energy will be reflected. Here, however, the shear waves propagating in the Ge rod used were not ideal planar waves, and nearly all of them have a small longitudinal component along the rod axis. If the rod diameter is small, they may be called the flexural waves [2-4]. This means that they strike the solid-liquid interface always with a slight

tilt. This tilt will cause mode conversion as shown in Fig.22.

The incident shear waves from the solid Ge will be partially reflected into one longitudinal and two shear waves, and partially transmitted into the longitudinal wave in the liquid Ge. The solid lines in Fig.22 indicate this process. When the longitudinal waves in the liquid Ge strike the liquid-solid boundary the mode conversion will also happen as indicated as the dashed lines. Although the longitudinal waves are generated during the mode conversion and reflected back to the shear wave transducer. No longitudinal arrivals has been observed, since the shear wave transducer is insensitive to longitudinal waves. Also because of the mode conversion longitudinal waves are propagating in the liquid Ge region, therefore the time delay will increase because of the slower velocity compared to that of shear waves in solid Ge. This agrees well with the above mentioned time delay observation in Fig.21.

As indicated in Section III.3 the acoustic impedance of the shear waves in the solid Ge is only about 1.2 times that of the longitudinal waves in the liquid. It is expected that a not-small amount of energy will be converted from the shear waves in the solid Ge into the longitudinal waves in the liquid Ge and vice versa. This is the reason why the echo reflected from the end of the rod can be observed even if it travels through the melt twice.

From Fig.21 it can be concluded that with the commercially available shear wave ultrasonic transducers water-cooled below 30 C the relative float zone position can be determined in a 10 mm diameter Ge rod oriented in the <100> direction and with a resolution of about 1 to 0.5 mm [27]. If the temperature profile along the Ge rod is known, then the velocity information listed in Table 4 may be used to determine the absolute position of the float zone.

The thickness of the float zone is also an important factor to determine the quality of the crystal growth. It may be determined by two methods as shown in Fig.23. The first is to use the two transducers geometry. Transducers 1 and 2 are able to obtain t1, t2 and tT. Since tT is equal to t1 + t2 + t_l , t_l which is the propagation time of the longitudinal waves through the liquid Ge (float zone) of thickness h can be obtained. Thus h can be obtained as h = t_l* v1, where v_l is equal to 2710 m/s [26]. The best resolution of this method is about twice of that of the moving float zone because it relys on the measurement resolutions of t1 and t2. Another method to obtain h is to use the multiple echoes of the longitudinal waves bouncing back and forth in the float zone as shown in Fig.23(b). The time delay will be equal to 2 t_l. From the recorded traces in Figure 21 it can be seen that this may be possible and this method potentially may provide better resolution. It should be noted that the thickness measured is an average value. At the present time no attempt has been used to find the shape of the liquid-solid Ge interface.

For the same experimental arrangements as those for Fig.21 many highly damped longitudinal Ultran transducers (2,5,10 MHz) were also tried, however the signal to noise ratio of the first longitudinal arrival was too poor for monitoring purposes. The conclusion is that since the diameter of the available Ge rod for the test is smaller than that of the ultrasonic longitudinal transducer, a very large amount of available signals is lost. This loss has been explained in Appendix A. Furthermore, the electrical shield of the Ultran transducers is not good. During the float-zone measurements heating results from by the high power RF signals which also cause a considerable amount of noise. More discussions related to longitudinal waves are given in Section VI.

V. CRYSTAL QUALITY

Because the float zone is a kind of crystal growth technique, one of the concerns is that ultrasound might disturb the crystal quality such as the dislocation density. If the product of the displacement of the propagating ultrasonic waves and the signal pulse repetition rate is less than the traveling speed of the float zone no deterious effects is expected. By comparing the crystal growth with and without the presence of the ultrasound, the difference will appear only if the ultrasonic disturbances are in phase. It means that the repeated ultrasonic waves strike the same atom at the liquid-solid interface before the float zone moves to the next atom.

In the experiments described in Section IV the float zone moved at a speed of 50 mm/hour which is equal to 3.5×10^5 Anstrons/sec. Assuming the ultrasonic displacement is 1 A°, the maximum repetition rate required to reach the moving speed of the float zone is 350 KHz which is much larger than 5 KHz used.

Another concern is that during the float zone process polycrystalline regions may be inadvertently formed if a polycrystal seed is initiated. Figures 24(a) and (b) show the transmitted and reflected signals using 12.7 mm diameter 2 MHz Ultran longitudinal Ultran transducers through a 9.5 mm diameter 292 mm long polycrystal Ge rod. It is clearly seen that the longitudinal signals are very messy due to the wave scattering at the crystalline boundaries indicating the possibility of detecting polycrystalline regions.

Figure 25 was the reflected signals obtained using a 2.25 MHz shear wave transducer performed on a 10 mm diameter 350 mm long polycrystal rod [27] during float zone refining. The recording procedures were the same as those described for Fig.21. At the lowest trace the rod is cold and signals are very messy like those in Figs.24 (a)&(b) for longitudinal waves. It is also seen that the reflected signal at the solid-liquid Ge interface is higher than the background scattered noises. Since the signals arriving prior to the interface echo do not change, the moving float zone may still be located if the difference between each

successive trace is monitored.

When a single crystal Ge rod is going through the float zone, its purity can be enhanced. The observation in Fig.25 offers a very interesting possibility that if a section of the rod is polycrystalline, the float zone can transform this section into a single crystal provided that the float zone moves from the single crystal to the polycrystalline section. The ultrasonic method may be used to monitor the presence of polycrystalline Ge by analysing the received signal conditions.

VI. CONCLUSIONS AND DISCUSSIONS

An ultrasonic pulse-echo method has been proposed to monitor the float zone in a Ge rod. The behaviors of acoustic wave propagation in anisotropic Ge were analyzed. In particular, effects of diffraction and mode conversion on received echoes of longitudinal and shear waves were described. Considerations and preliminary results related to high temperature ultrasonic measurements were presented. The potential feasibility of this method has been experimentally demonstrated by using shear wave transducers cooled at about 30°C with small diameter Ge rods. It was shown that arrival times and amplitudes of the reflected signals from the solid-liquid Ge interface can be used for monitoring purposes and good resolution can be obtained for both zone position and thickness. Acoustic energy transfer at the solid-liquid interface, observed even in the case of shear waves, was discussed in terms of mutiple mode conversion.

One concern in this project is the actual size of the Ge rod if the float zone method is performed in space. The diameter and the length of the Ge rod directly affect the ultrasonic method. For instance, can water-cooling be used for such rods in space? What is the actual temperature at the rod end? It is discussed in Section III that the elevated temperature not only limits the available transducers but also the coupling materials, the transducer backing materials (for damping purpose), electrical connection methods between the transducer and the electronic instruments, etc.

The proposed future studies for this project are

1. to use the water-cooled and less damped longitudinal transducers such as those from KB-Aerotech to monitor the float zone of a single crystal Ge rod with its diameter larger than that 12.7 mm (common diameter of ultrasonic transducers). The signal to noise ratio is 20 dB higher if KB-Aerotech longitudinal transducers are used compared to Ultran transducers.

2. to test the coupling materials, electrical connections of the ultrasonic transducers and backing materials for high temperature operation for both longitudinal and shear waves.

3. to try more signal processing methods to analyzed the

obtainable data [27].

4. to find any other alternative method.

ACKNOWLEDGEMENT

The technical assistance of D. Hardy and P. Sutcliffe of CAL and the helpful discussions with L. Piche of IMRI are greatly appreciated. The authors also acknowledge the experimental preparation of float zone ultrasonic measurement by R. Beauprie and S. Willson of Cominco Ltd.

REFERENCES

[1] J.E. May, IRE Trans. Ultrasonics Eng., Vol.UE-7, PP.44, 1960.

[2] A.H. Meitzler, "Mode coupling occurring in the propagation of elastic pulses in wires", J. Acoust. Soc. Am., Vol.33, pp.435-445, 1961.

[3] J. Zemanek, Jr., "An experimental and theoretical investigation of elastic wave propagation in a cylinder", Ph.D. dissertation, UCLA, California, 1962.

[4] T.R. Meeker and A.H. Meitzler, "Guided Wave Propagation in Elongated Cylinders and Plates", Physical Acoustics, Vol.I, Part A, Academic Press, Chapter 2, pp.111-167, 1964.

[5] I. Mirsky, "Wave propagation in transversely isotropic circular cylinders", Part I & II, J. Acoust. Soc. Am., Vol.37, pp.1016-1026, 1965.

[6] F.C. Eliot and G. Mott, "Elastic waves propagation in circular cylinders having hexagonal crystal symmetry", J. Acoust. Soc. Am., Vol.44, pp.423-430, 1968.

[7] L.O. Wilson, " Wave propagation along a sapphire rod", J. Acoust. Soc. Am., Vol.61, pp.995-1003, 1977. Also "Vibrations of a lithium niobate fiber", Bell Syst. Tech. J., Vol. 1977.

[8] B.A. Auld, "Acoustic Fields and Waves in Solid," John Wiley & Sons, Vol.I, Chap.7. pp.265-348, 1973.

[9] C.K. Jen, 'Introduction to engineering ultrasound', Technical Report, NRCC IGM-86-401-03, June 1986.

[10] P.C. Waterman, "Orientation dependence of elastic waves in single crystals", Phys. Rev., Vol.113, pp.1240-1253, 1959.

[11] E.P. Papadakis, 'Diffraction of ultrasound radiating into an elastically anisotropic medium', J. Acoust. Soc. Am., Vol.36, pp.414-422, 1964.

[12] E.P. Papadakis, 'Ultrasonic diffraction loss and phase change in anisotropic materials', J. Acoust. Soc. Am., Vol.40, pp.863-876, 1966.

[13] M.G. Cohen, "Optical study of ultrasonic diffraction and focusing in anisotropic media", J. Appl. Phys., Vol. 38, pp.3821-3828, 1967.

[14] D.L. Hecht and G.W. Petrie, "Acousto-optic diffraction from acoustic anisotropic shear modes in gallium phosphide", Proc. IEEE Ultrasonics Symp., pp.474-479, 1980.

[15] C.K. Jen, G.W. Farnell, E.L. Adler and J.A. Oliveira:

'Interactive computer-aided analysis for bulk acoustic waves in materials of arbitrary anisotropy and piezoelectricity', IEEE Trans. on Sonics and Ultrason., Vol.SU-32, pp.56-60, Jan. 1985.

[16] E.R. Dobbs, B.B. chick and R. Truell, "Attenuation of sound in a germanium crystal at ultra-high frequencies and low temperatures", Phys. Rev. Lett., Vol.3, pp.332-334, 1959.

[17] W.P. Mason and H.J. McSkimin, "Attenuation and scattering of high frequency sound waves in metals and glasses", J. Acoust. Soc. Am., Vol.19, pp.464-473, 1947.

[18] H.J. McSkimin, "Propagation of longitudinal waves and shear waves in cylindrical rods at high frequencies", J. Acoust. Soc. Am., Vol.28, pp.484-494, 1956.

[19] L.M. Brekhovskikh, "Waves in layered media", 2nd ed., Academic Press, New York, 1980. p.13.

[20] E.P. Papadakis, "Effects of input amplitude profile upon diffraction loss and phase change in a pulse echo system", J. Acoust. Soc. Am., Vol.49, pp.166-168, 1971.

[21] A.H. Meitzler, "Ultrasonic Transducer Materials," edited by O.E. Mattiat, (Plenum, New York, 1971), Chap.3. pp.125-182.

[22] H.J. McSkimin, 'Measurement of ultrasonic wave velocities and elastic moduli for small solid specimens at high temperatures', J. Acoust. Soc. Am., Vol.31, pp.287-295, 1959.

[23] G. Simmons and H. Wang, 'Single crystal elastic constants and calculated aggregate properties: a handbook', 2nd ed, MIT Press, Mass., 1970.

[24] Y.A. Burenkov, S.P. Nikanorov and A.V. Stepanov, 'Elastic properties of germanium', Sov. Phys. Solid State, Vol.12, pp.1940-1942, 1971.

[25] V.M. Glazov, A.A. Aivazov and V.I. Timoshenko, 'Temperature dependence of the velocity of sound in molten germanium', Sov. Phys. Solid State, Vol.18, pp.684-685, 1976.

[26] R.L. Parker and J.R. Manning, "Application of pulse-echo ultrasonics to locate the solid/liquid interface during solidification and melting", J. Crystal Growth, Vol.79, pp.341-353, 1986.

[27] Ph. de Heering, "Acoustic float zone sensing", contract report, March 1988.

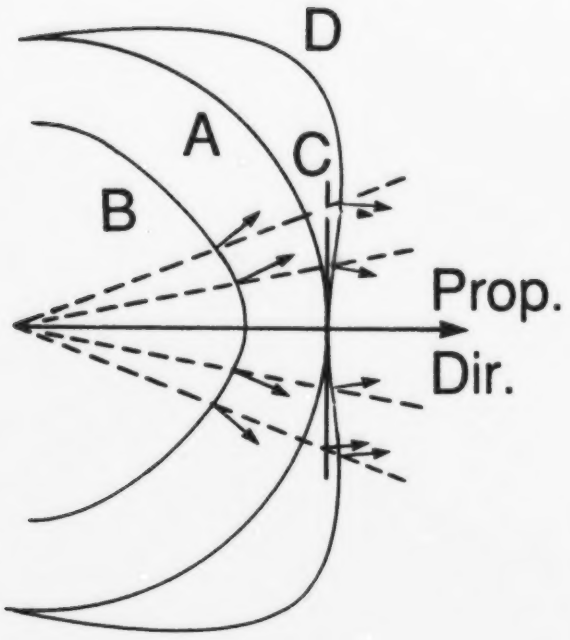

Fig.1 Some typical slowness curves. Curve A in is an isotropic case and B, C and D exhibit diverging, collimating and focusing behavior respectively.

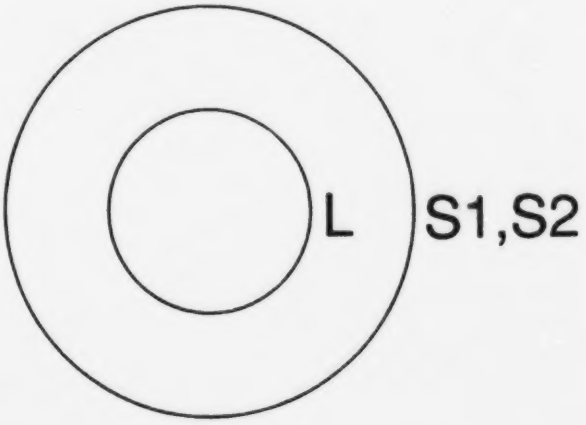

Fig.2 The slowness curves of an isotropic Al.

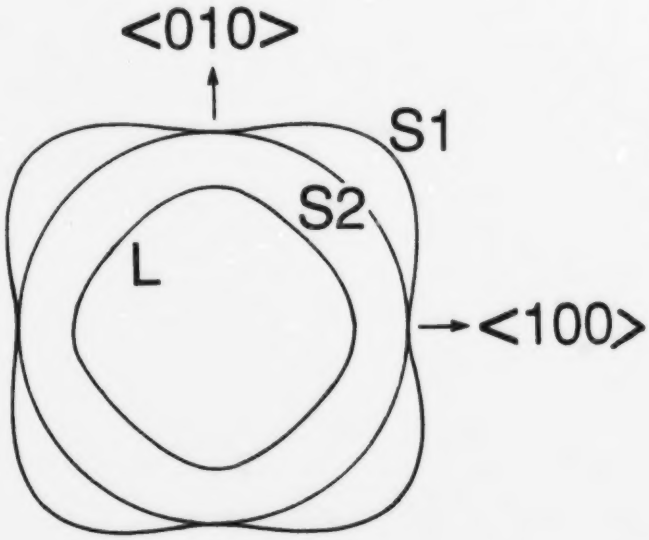

Fig.3 The slowness curves of Ge crystal in the <100> [001] plane.

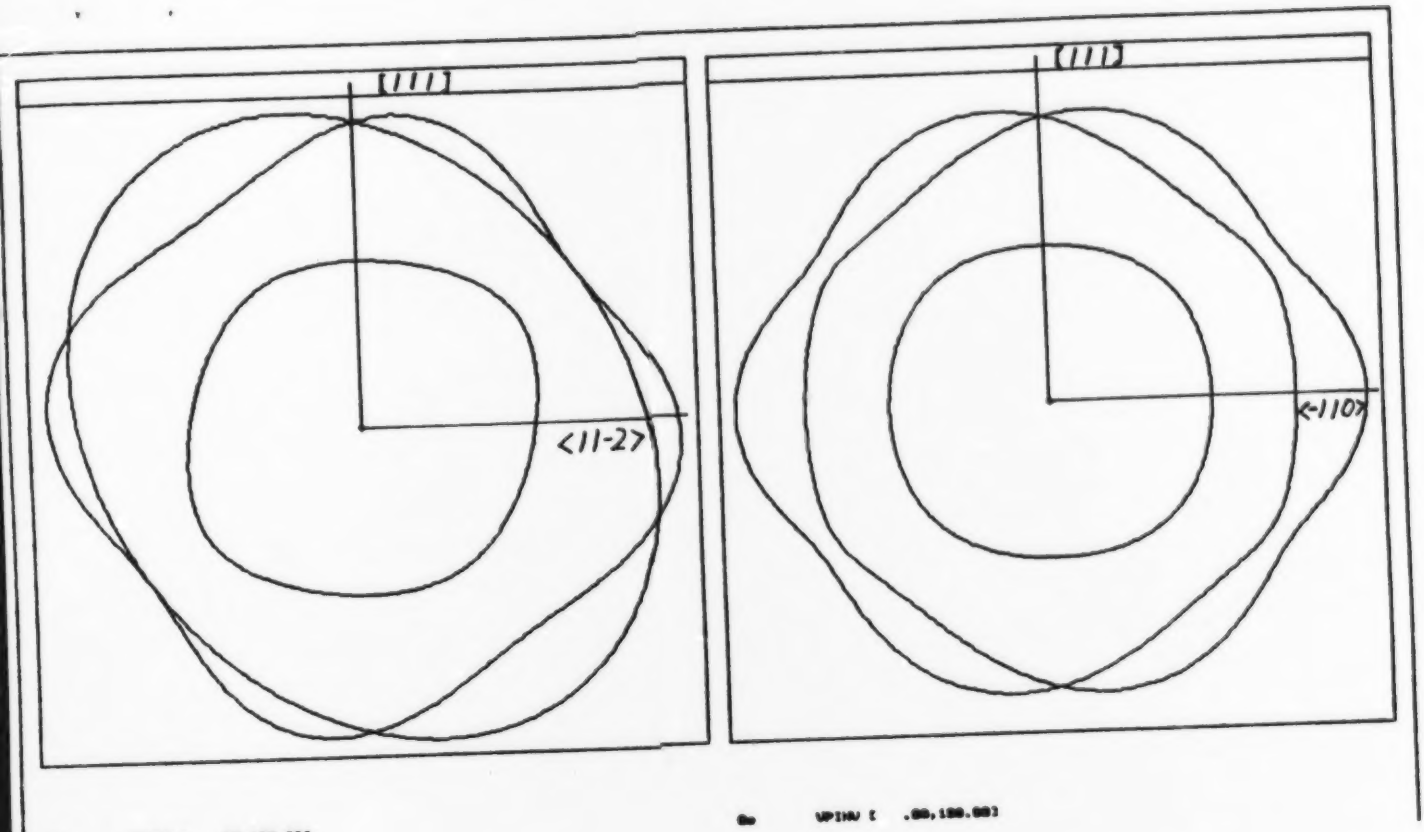

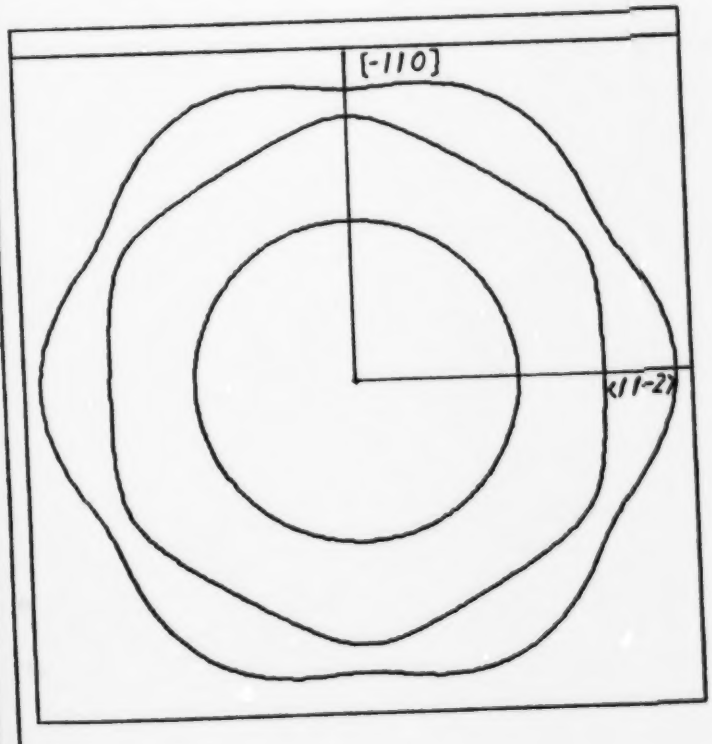

Fig.4 The slowness curves of Ge in the B(a) <11-2> [111], (b) <-110> [111] and (c) <11-2> [-110] planes.

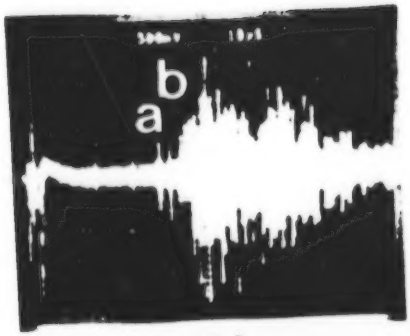

(a)

Fig.5

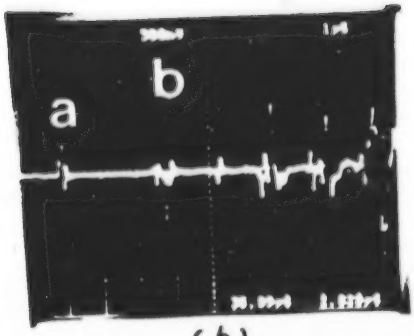

(b)

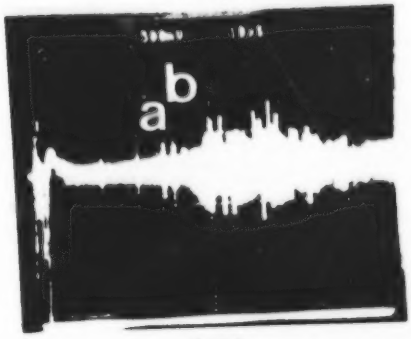

(a)

Fig.6

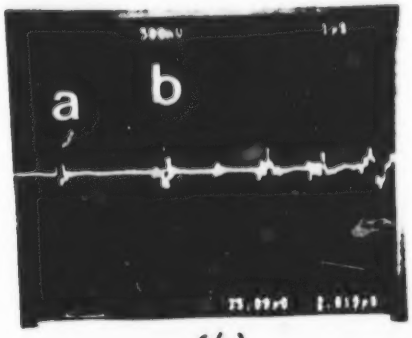

(b)

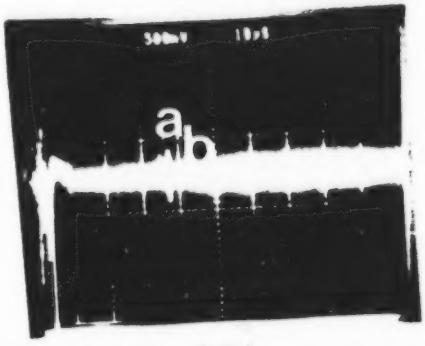

(a)

Fig.7

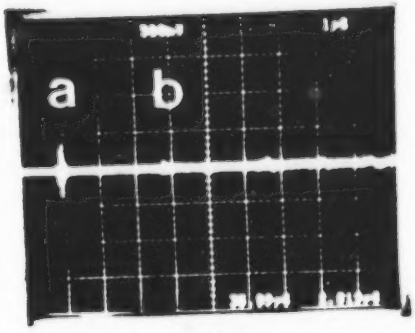

(b)

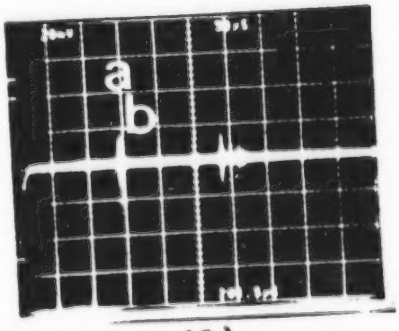

(a)

Fig.8

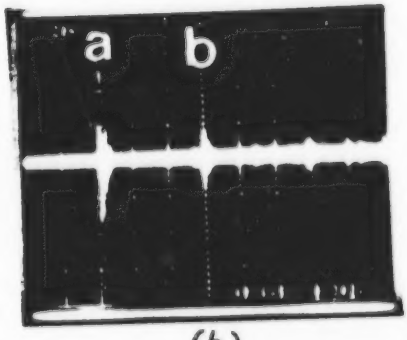

(b)

Fig.5-8 (a)&(b) The reflected echoes at the back surface of a Ge rod with a 10 mm diameter and 91.0 (Figs.5-7) or 340 mm (Fig.8) length using 5 MHz (12.7 mm dia), 5 MHz (6.35 mm dia.) and 15 MHz (4.57 mm dia. Figs.7&8) Ultran longitudinal transducers respectively. (b) is the zoomed picture of (a). The rod axis is along <100> direction.

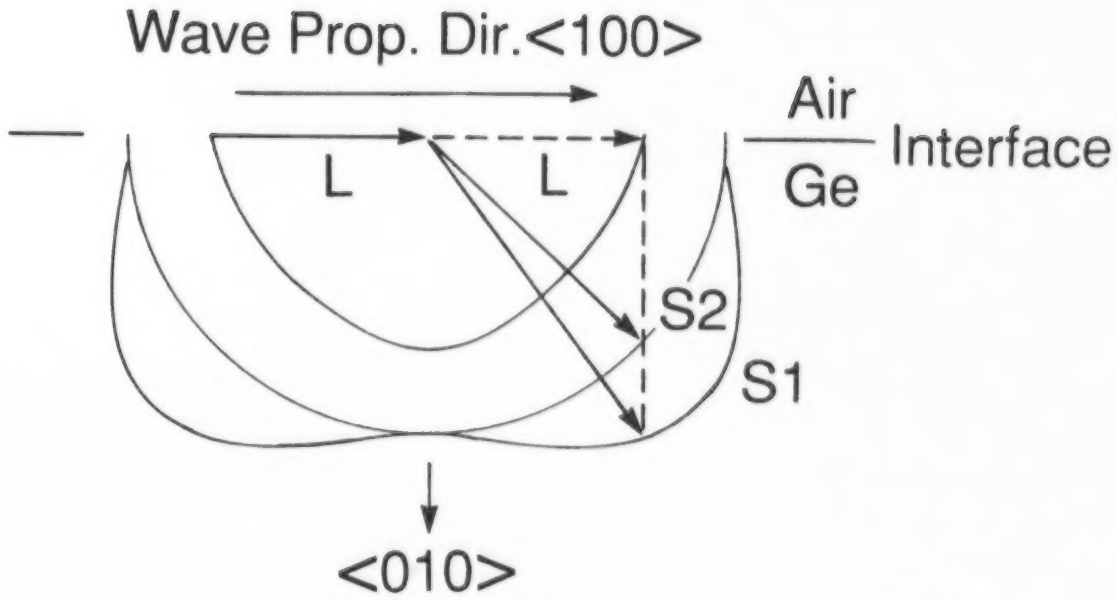

Fig.9 Phase matching requirements represented with the slowness curves of Ge <100> [001] plane for the mode conversion process.

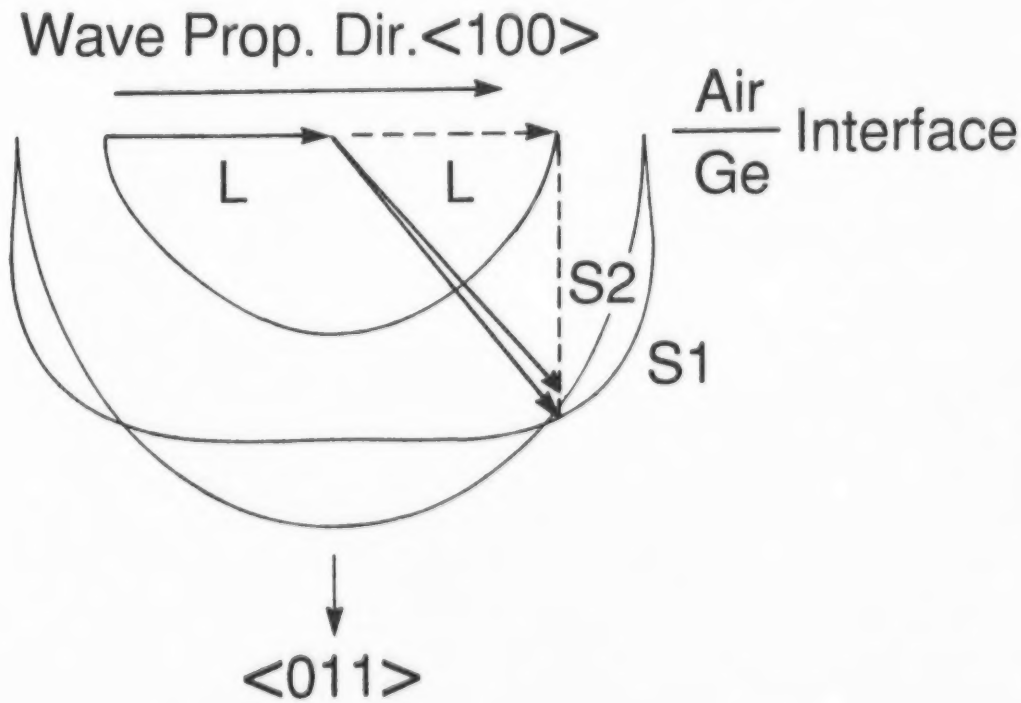

Fig.10 Phase matching requirements represented with the slowness curves of Ge <100> [011] plane for the mode conversion process.

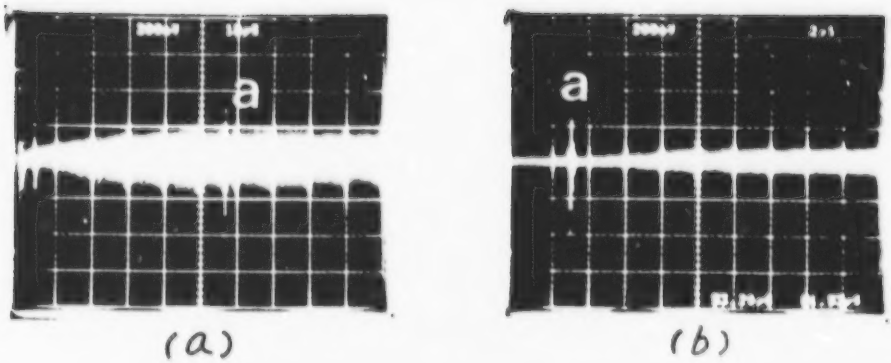

Fig.11 (a) The received signals from the end of a 156 mm long and 14 mm diameter Ge rod whose rod axis is the <111> orientation using a 15 MHz 4.57 mm diameter Ultran longitudinal transducer in the reflection geometry. (b) is the zoomed picture of (a).

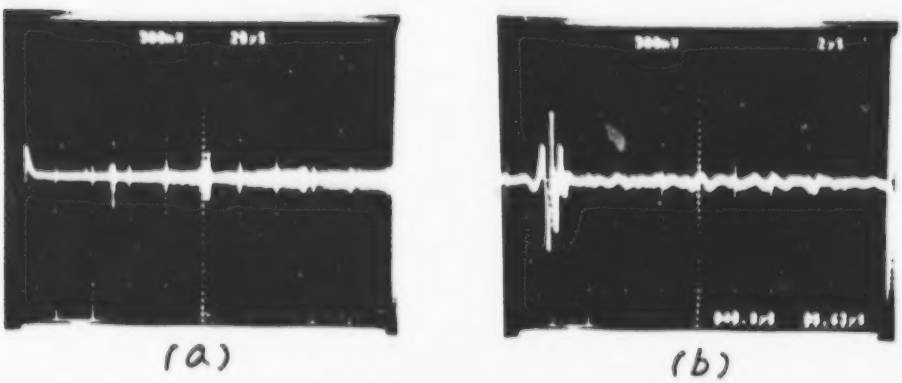

Fig.12 (a) The received reflected signal from a 10 mm diameter, 91 mm long Ge rod with the rod axis oriented in <100> direction using a 2.25 MHz Panametrics shear transducer with 12.7 mm diameter. (b) is the zoomed picture of (a).

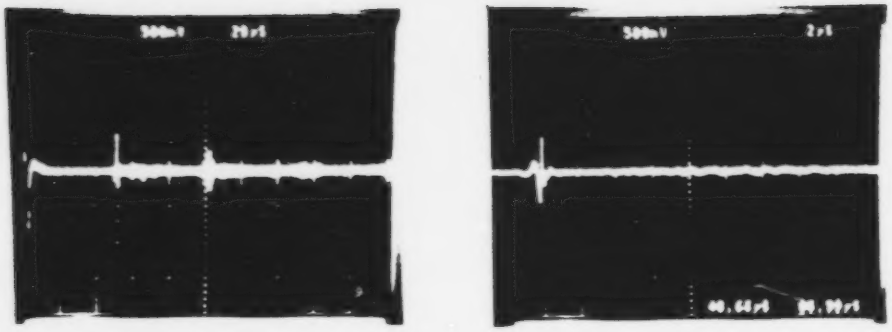

(a) (b)

Fig.13 (a) The received reflected signal from a 10 mm diameter, 91 mm long Ge rod with the rod axis oriented in [100] direction using a 5 MHz Panametrics shear transducer with 12.7 mm diameter. (b) is the zoomed picture of (a).

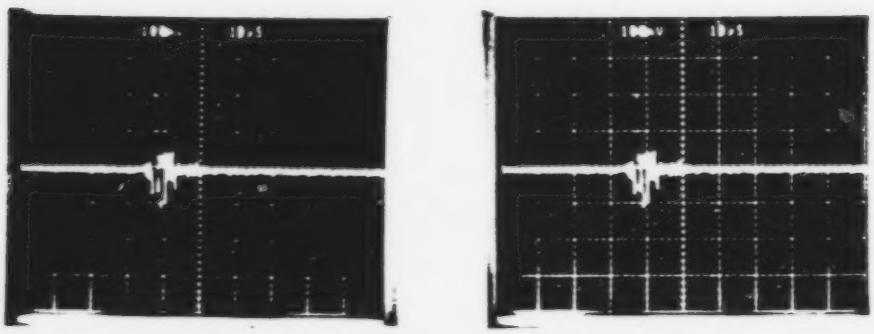

(a) (b)

Fig.14 The transmitted shear wave arrivals for a 14 mm diameter 101 mm long Ge rod oriented in the <111> direction.

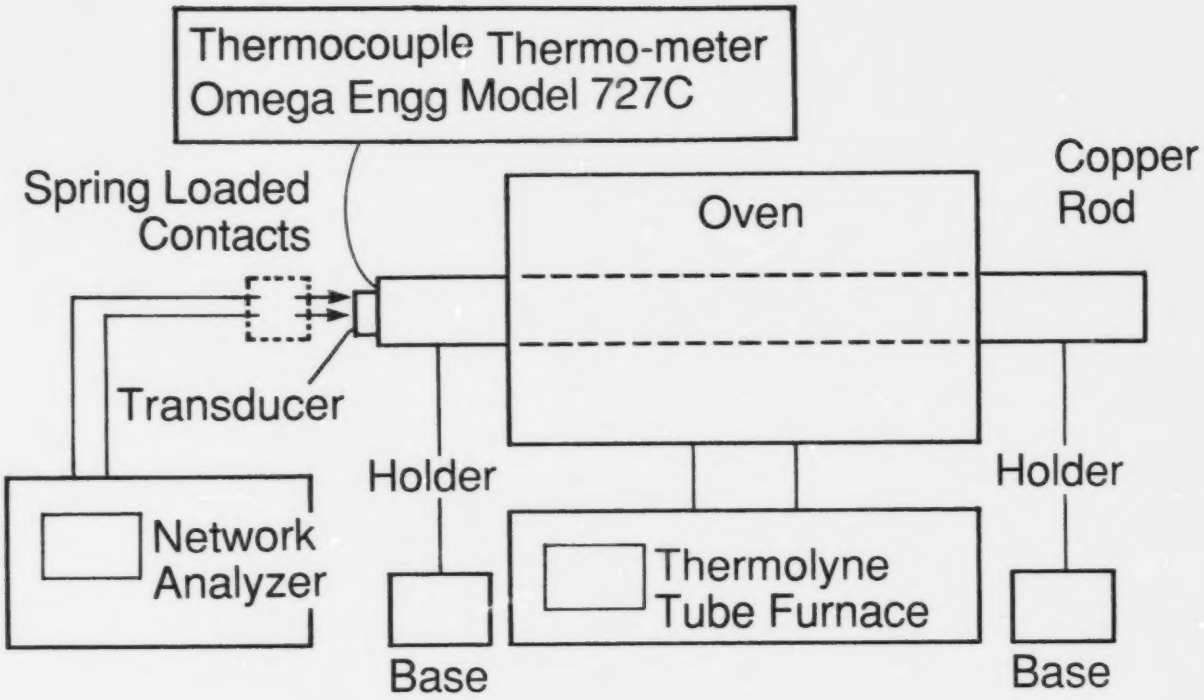

Fig.15 The experimental setup for the high temperature test of thin disc LiNbO3 transducers.

Fig.16 Spring loaded type connector spot welded to a BNC connector.

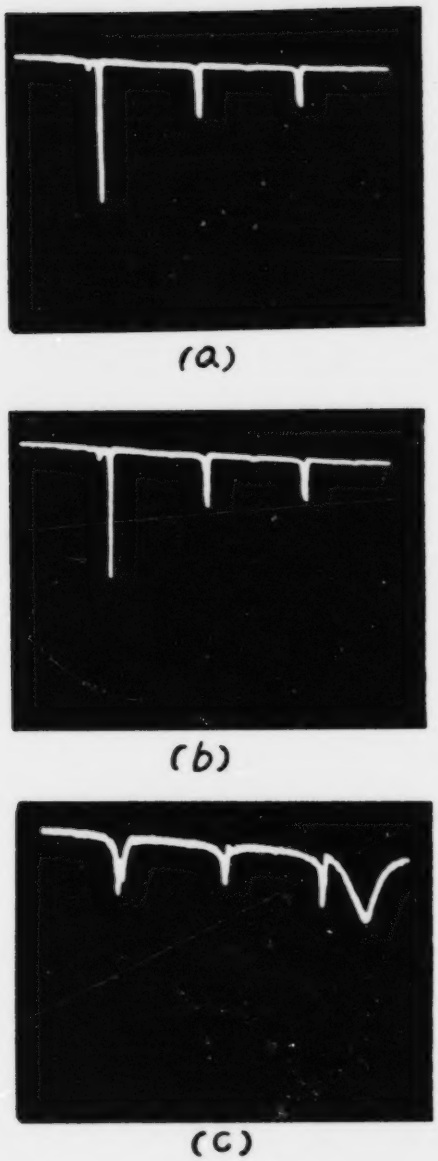

Fig.17 The reflected signal of a LiNbO3 transducer performed at (a) 25, (b) 419 and (c) 502°C using a HP8754A Network Analyzer. The horizontal axis is the frequency.

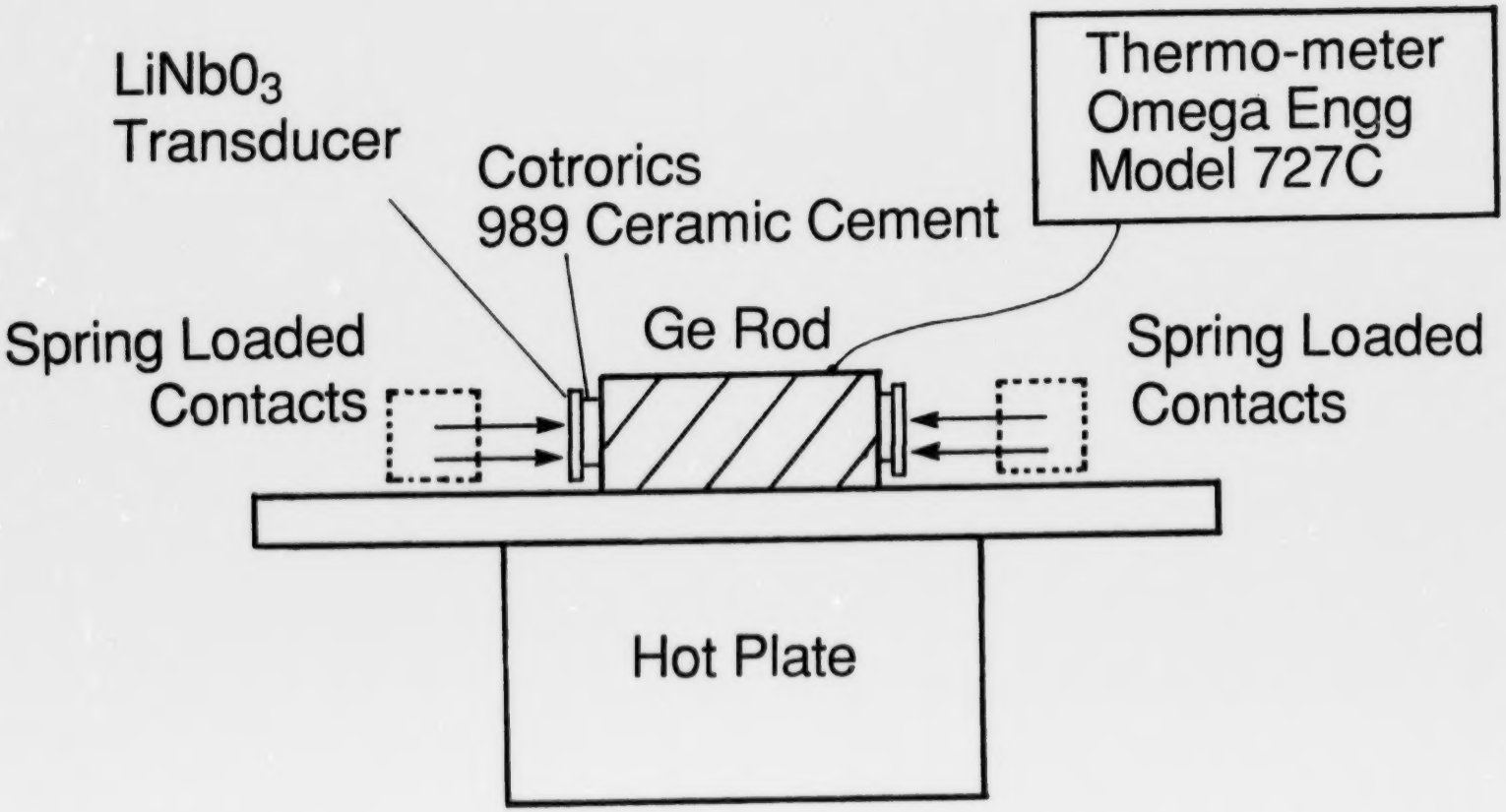

Fig.18 The experimental setup for the ultrasonic test of the coupling cement at elevated temperatures.

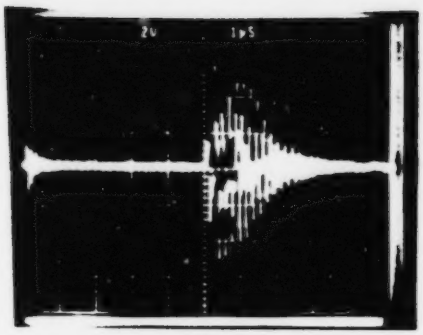

(a)

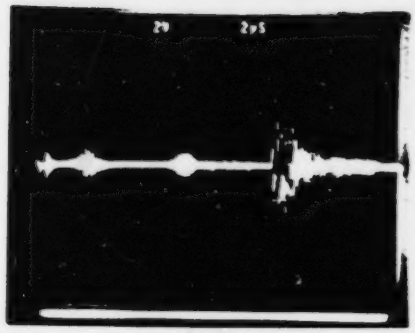

(a)

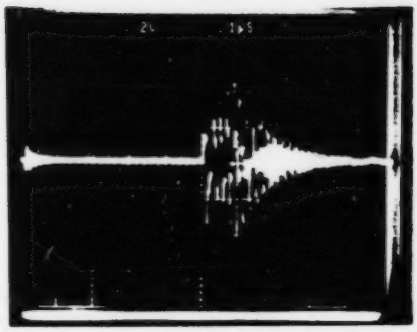

(b)

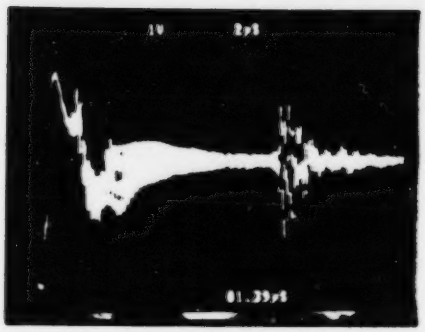

(b)

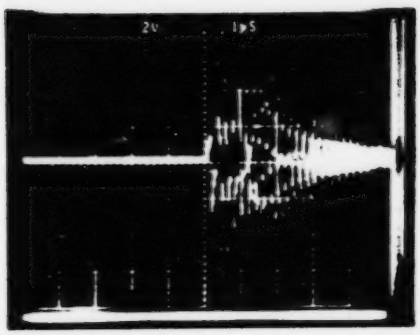

(c)

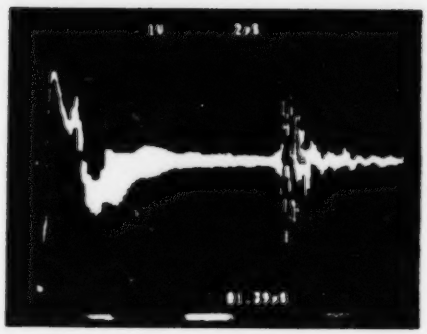

(c)

Fig.19 The transmitted longitudinal signals through a 10 mm diameter 27 mm long Ge rod using a pair of 5 MHz longitudinal disc $LiNbO_3$ transducer with a 6.35 mm diameter at (a) 25, (b) 200 and (c) 350° C.

Fig.20 The reflected shear wave signals through a 10 mm diameter 20 mm long Ge rod using a 5 MHz shear wave transducer with a 6.35 mm diameter at (a) 25, (b) 200 and (c) 350° C.

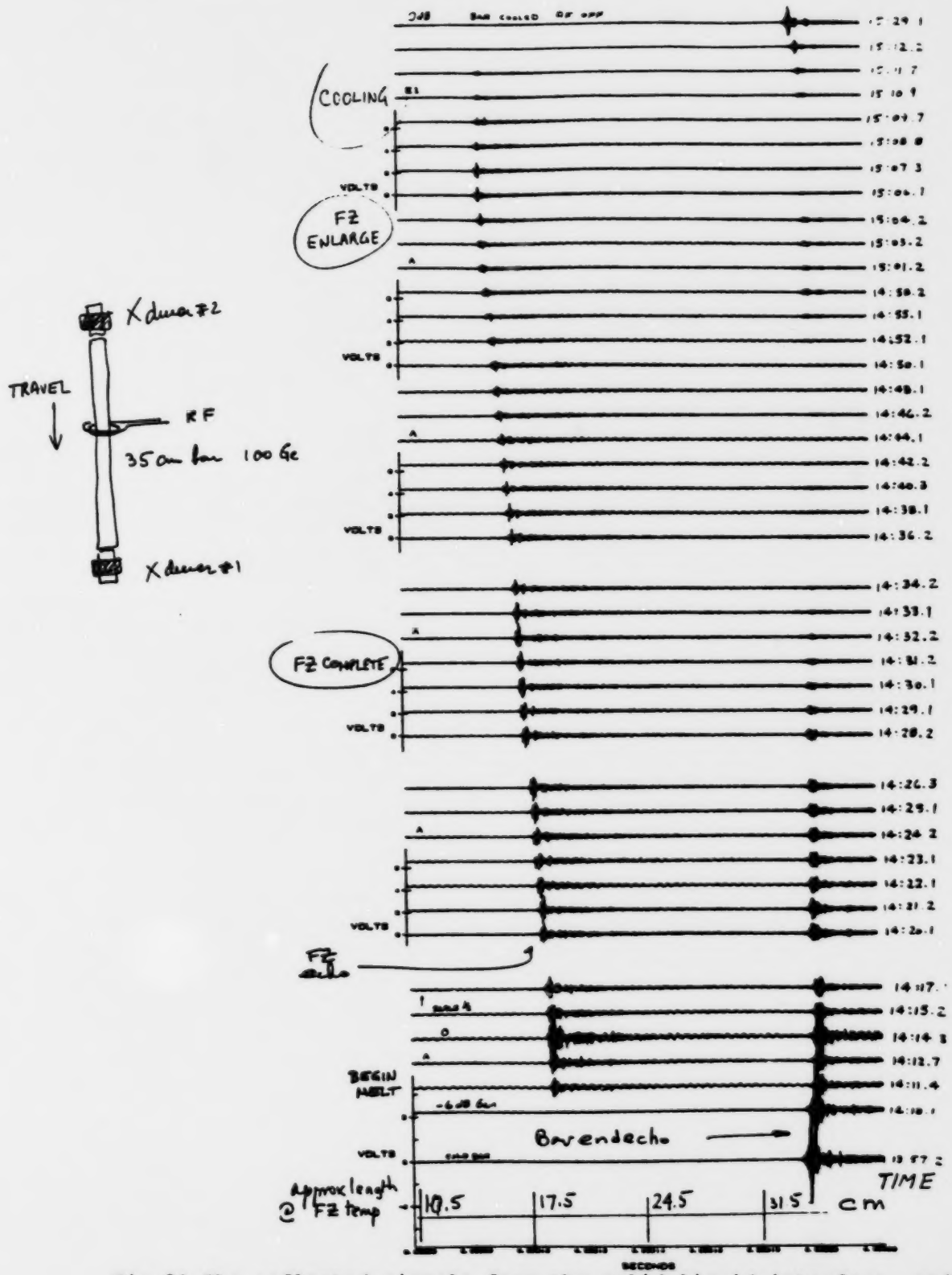

Fig.21 The reflected signals from the solid-liquid interface and the end of the rod with a 5 MHz, 12.7 mm diameter shear wave transducer performed on a 10 mm diameter 350 mm long Ge rod oriented in the <100> direction during the float zone experiment. [27]

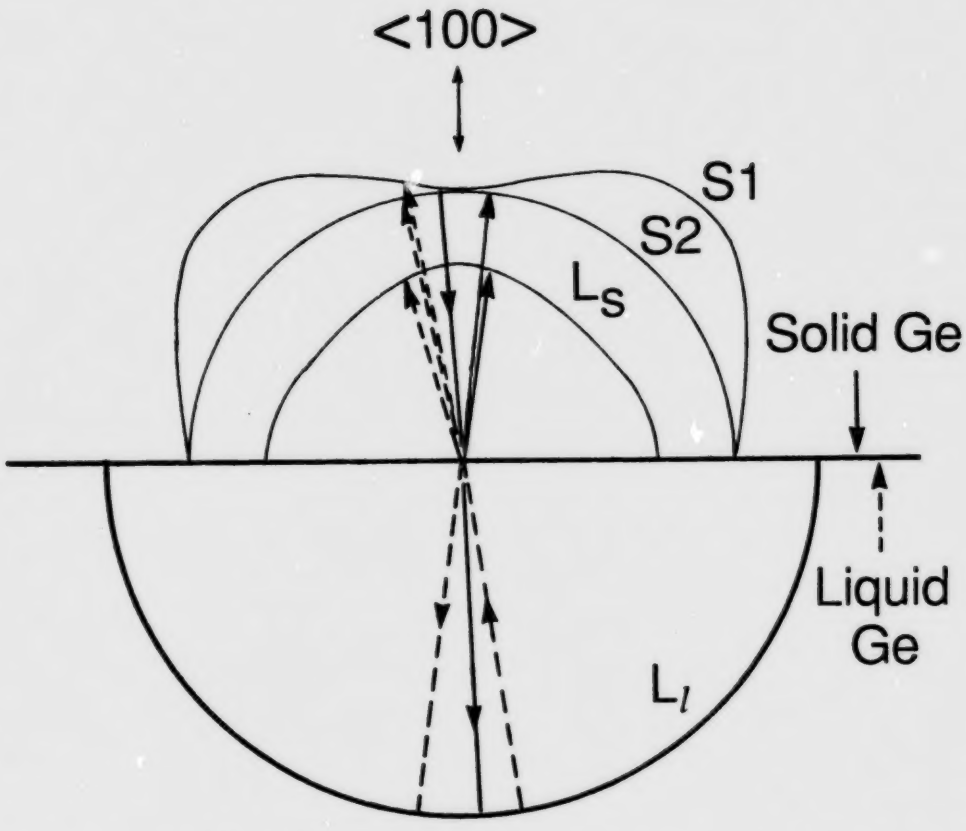

Fig.22 Multiple mode conversion processes at the solid-liquid interface of a Ge rod with its axis oriented in the <100> direction.

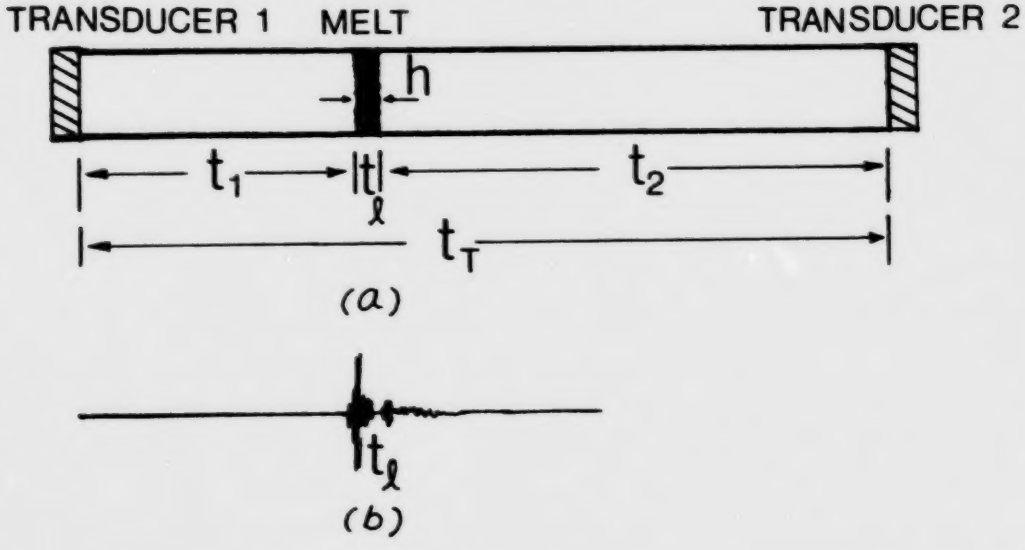

Fig.23 (a) and (b) Two methods to determine the thickness of the float zone.

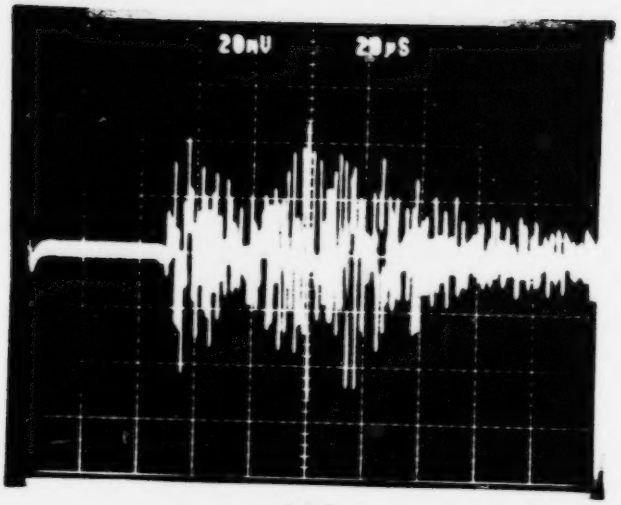

(a)

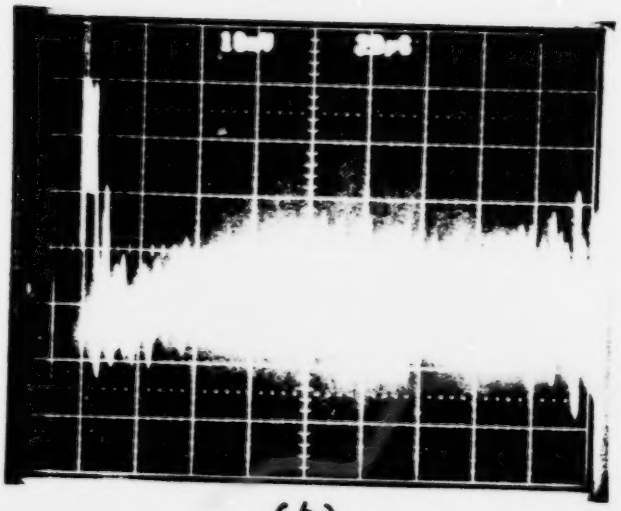

(b)

Fig.24 (a) The transmitted and (b) reflected signals using 12.7 mm diameter 2 MHz Ultran longitudinal Ultran transducers through a 9.5 mm diameter 292 mm long polycrystal Ge rod.

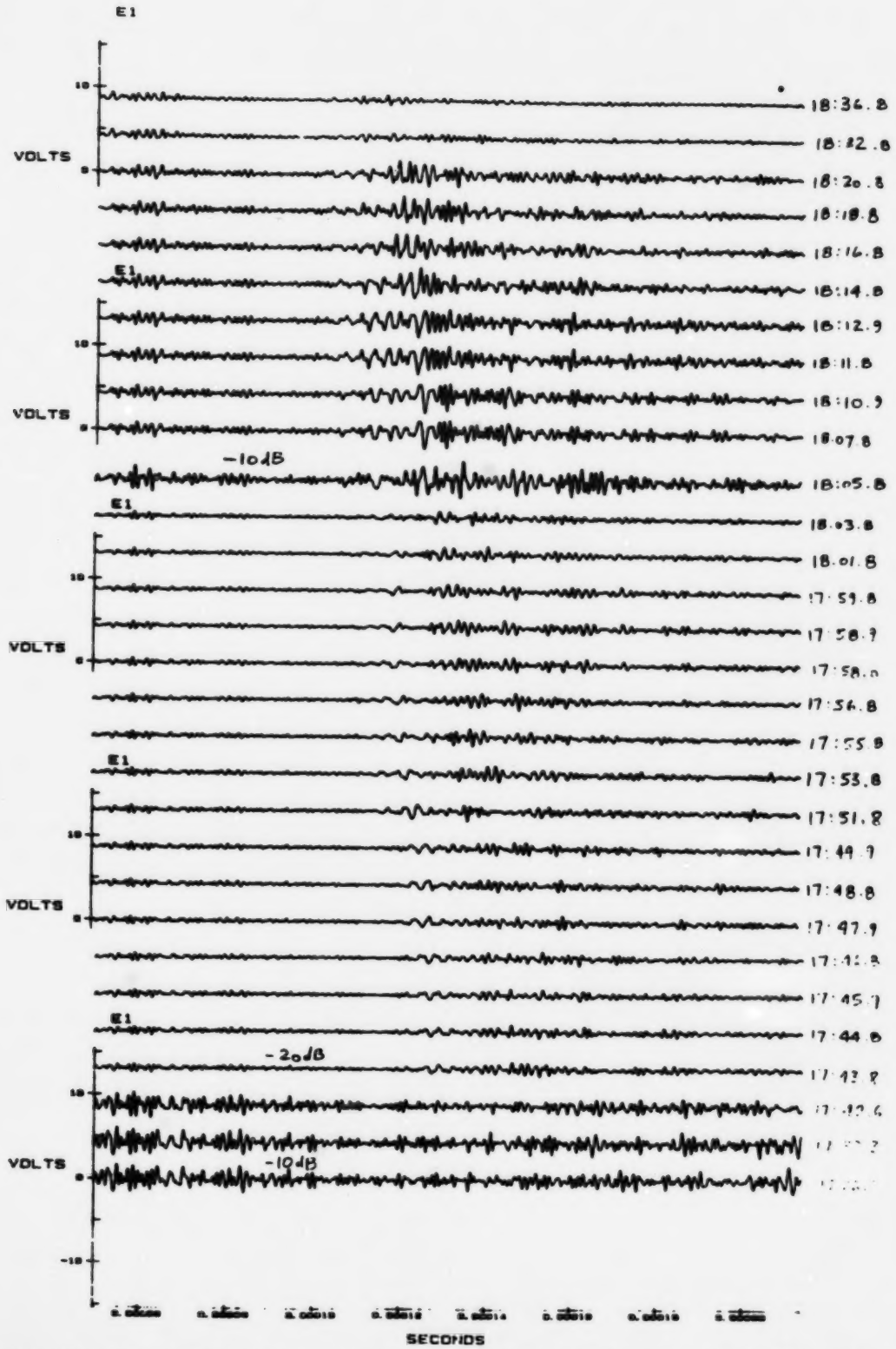

Fig.25 The reflected signals obtained using a 2.25 MHz shear wave transducer performed on a 10 mm diameter 350 mm long polycrystal rod [27].

APPENDIX A ACOUSTIC WAVE PROPAGATION IN ALUMINUM RODS

I. Longitudinal Waves

Longitudinal acoustic wave measurements have been performed using aluminum (Al) rods with different diameters and lengths shown in Fig.A1 in the transmission or reflection geometry. Table A1 gives the descriptions of these Al rods. Many transducers with different operating frequencies and apertures were also used. Here only a few figures related to the project are given.

TABLE A1 Descriptions of AL Rods

Type	Diameter (mm)	Length (mm)	Remarks
A	12.7	220	uniform diameter
B	12.7	218	one end with smaller diameter (dia. 8.50 mm, length 28 mm)
C	12.7	219	both ends with smaller diameters (dia. 7.71 mm, length 33 mm and dia. 8.35 mm, length 31 mm)
D	12.7	219	both tapered ends (dia. 6.12 mm, length 34 mm and dia. 5.97 mm, length 34 mm)
E	12.7	219	notch at the center (notch depth 4.0 mm)
F	12.7	220	notch at one-third (notch depth 4.0 mm)
G	12.7	110	uniform diameter
H	12.7	55	uniform diameter
I	7.95	222	uniform diameter
J	19.0	219	uniform diameter
K	19.0	206	periodic notches (notch depth 3.15 mm)
L	19.0	213	double spiral notches (notch depth 3.15 mm)
M	19.0	85	uniform diameter

Figures A2 and A3 show the transmitted and reflected echoes through the Al Rod 'A' using a 5 MHz Ultran transducer with a 12.7 mm diameter. The echo 'a' is the first longitudinal arrival. Echoes 'b', 'c' etc arrive later than 'a' and the time delays td's between 'a' and 'b', 'b' and 'c', 'c' and 'd' etc are nearly equal. Echoes 'a', 'b' and 'c' for Al rods 'A', 'C', 'D', 'E', 'F', 'H', 'I' and 'J' obtained in the transmission geometry are given in Figures A4 (a)-(h) respectivley. The amplitudes in Figures A4 are arbitrary, but the received amplitude of echo 'a'

for Al rods 'I', 'A' and 'J' using the above mentioned transducer are -40, -6 and 0 db respectively. From Figures A4 the following observations have been noticed.

1. Time delays between the trailing echoes are nearly equal.

2. The time delay td is proportional to the rod diameter (see (g), (a) and (h)) but not the length (see (a)&(f)). A rod having two diameters displays two different td's (see (b)). The ratio of these two td's is the same of that of the corresponding diameters.

3. One notch at the center ('E') of the rod or off center ('F') or tapering the rod end ('D') does not affect the td (see (d),(e) & (c)).

The presence of trailing echoes was reported in Refs. [17,18], but no attempt was made to evaluate td. In fact, the cause of the time delay td can be explained by a mode conversion process illustrated in Figs.A5(a)&(b). The longitudinal waves travelling almost parallel to the rod-air interface but with a small angle of inclination impinge on the interface and induce mode conversion from longitudinal (L) to shear waves (S). The roughness of the surface also enhances this conversion. It is noted that there are two shear waves with orthogonal particle polarizations in Fig.A5(a), and because they are degenerate (i.e. having the same velocity), they are represented by a single curve. The mode conversion is dictated by the phase matching requirements shown in Fig.A5(a), therefore the θ in Fig.A5 is equal to $\sin^{-1}(vs/vl)$. vs and vl are the shear (3109 m/s) and longitudinal wave velocity (6420 m/s) of the Al. The phase matching condition requires that the wavenumber components of the waves involved in the mode conversion along the interface must be equal [8,9]. When the converted shear waves strike the other side of the rod-air interface, they are converted back to longitudial waves because the phase matching conditions still hold. This can be seen if the directions of the arrows in Fig.A5(a) are reversed. Thus from the the propagation paths of echo 'a' and 'b' shown in Fig.A5(b) td which is the arrival time delay difference between echoes 'a' and 'b' can be expressed as

$$t_d = \frac{d/\cos\theta}{vs} - \frac{d*\tan\theta}{vl} \qquad (A.1)$$

where d is the diameter of the rod

Using Eqn.(A.1) the calculated and the measured td between echoes 'a' and 'b' shown in Figs.4(a), (g) and (h) are 3.57 and 3.60, 2.24 and 2.25, 5.34 and 5.40 μs respectively. The agreement is excellent. In addition, the echoes 'b' and 'c' etc are the sources of echoes 'c' and 'd' etc respectively, therefore the time differences between these trailing echoes are nearly the same. Since mode conversion process happens continuously along the rod, the narrow notches or the length do not affect the time

td. The three obervations mentioned above have been explained consistently by the mode conversion process.

The trailing echoes 'b', 'c' etc are the result of the wave diffraction in the rod. The ratio between the energy sum of all trailing echoes over that of the first arrived longitudinal echo 'a' may be used to evaluate the degree of diffraction in the rod. In order to reduce this ratio one obvious method is to increase the diameter or shorten the length of the rod. Another alternative is to disturb the rod-air boundaries as the rod 'L' shown in Fig.A1. Rod 'L' was made in a way that a spiral like V grooves with a depth of 3.15 mm are surrounding the rod. The diameter of the untouched portion inside the rod 'L' is 12.7 mm which is the same as that of rod 'A'. The spiral directions consist of both clockwise and counter-clockwise so that no cylindrical symmetry can be found along the rod. This boundary not only destroys but also absorb a major portion of the diffracted waves due to the effective imaginary acoustic impedance [19]. This reduction of trailing echoes is clearly illustrated by comparing the the reflected echoes through the Al rod 'L' in Figs.A6(a)&(b) with those through the Al rod 'A' in Fig.A3 using a 5 MHz Ultran transducer with a 12.7 mm diameter.

The increase of the acoustic operating frequency can also reduce the diffraction effect [11,12], hence this ratio. The particle velocity profile across the face of a transducer has been also shown to have large effects upon the diffraction [20]. By comparing the received signals in Figures A7(a)&(b) obtained with a 25 MHz and 6.35 mm diameter KB-AEROTECH transducer and those in Figure A3 obtained with a 5 MHz and 12.7 mm diameter Ultran transducer performed on the same rod 'A', it can be said that the diffraction effect of the former case is much less than that of the latter. Fig.A8(a)&(b) show the reflected signals with a 25 MHz and 6.35 mm diameter KB-AEROTECH transducer from the end of the rod 'L'. The trailing echo 'b' is more than 30 db smaller than that of the first longitudinal arrival echo 'a'.

In the ultrasonic measurements let p and q be the diameter of the rod and the transducer respectively. Assuming there is no loss in the rod, the received signals may be proportional to $20 \log[(p/q)^4]$. The expected signal amplitude of echo 'a' for rod 'H', 'A' and 'J' are 0, 0 and -16 db, however the measured values are 0, -6 and -34 db respectively. The causes for the extra reduction in signal levels may be due to that the longitudinal waves in the thin rod are becoming flexural in nature [2-4]. This means that a transverse component will exist together with the longitudinal component of particle displacement. More propagating longitudinal waves will have some inclination when they strike the rod-air boundary. This results in an increase of the mode conversion, thus also a decline of the signal level of 'a'. Furthermore, the efficiency of the longitudinal transducer to excite flextural modes are less than the longitudinal modes.

II. Shear Waves

Shear wave measurements were made using a 12.7 mm diameter Panametrics transducers with different center frequencies. Figures A9-11(a)&(b) were obtained by a 5 MHz transducer performed with the rod 'I', 'A' and 'J' respectively in the reflection geometry and Figure A12 with a 2.25 MHz transducer performed with the rod 'A'. It is noted that in each (a) the mutiple echoes are coming from the end of the rod and no trailing echoes such as mentioned in the previous section are observed.

When the shear waves travelling nearly parallel to the rod-air interface strike the interface, the phase matching requirements indicate that they can not have the kind of mode conversion process which induce the dominant trailing pulses like those observed in the longitudinal wave measurements. This is clearly verified in Figs.A9-A12.

It is also interesting to note that the high frequency components of the first longitudinal echo arrive earlier than the low frequency components for all Al rods listed in Table A1. In shear wave measurements this is true only for Figs.A9 and A12 but not for Figs.A10 and A 11. The reason for this is not understood at present.

The reflected shear wave signals from the end of rod 'A' and rod 'J' are similar level. However, the reflected signals from the rod 'L' is not only more than -40 db lower in signal level but also very messy. The reduction in signal level seems mainly due to the aborption mechanism of the periodic grooves mentioned earlier, but the for the difference in absorption between the longitudinal and shear incident waves is not understood. The messy signals are due to the reflections from the grooves.

In all the shear wave measurments performed on the long Al rods with a 2.25 or 5 MHz transducer the received signals are very sensitive to the boundary conditions. For instance hand pressure at the rod periphery will change signal levels by about 5 db. This does not appear at all in the longitudinal wave measurements. From all the results obtained it is ,therefore, concluded that for the same acoustic wavelength the diameter of the Al rod for shear wave propagation should be much larger than that of the longitudinal waves.

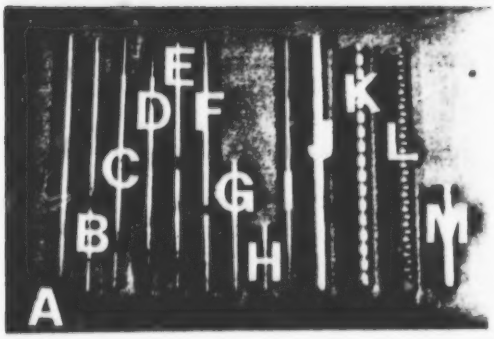

Fig.A1 Al rods used in the measurements.

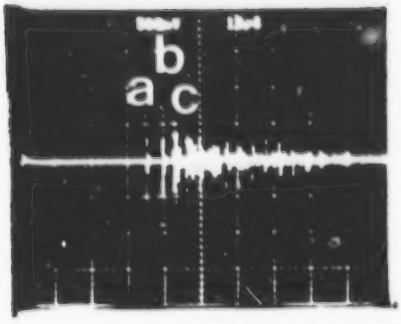

Fig.A2 The transmitted echoes through the Al Rod 'A' using a 5 MHz Ultran longitudinal transducer with a 12.7 mm diameter.

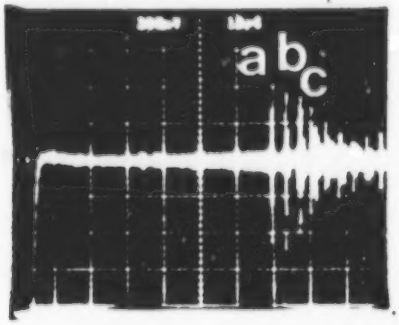

Fig.A3 The reflected echoes through the Al Rod 'A' using the transducer describe in Fig.A2.

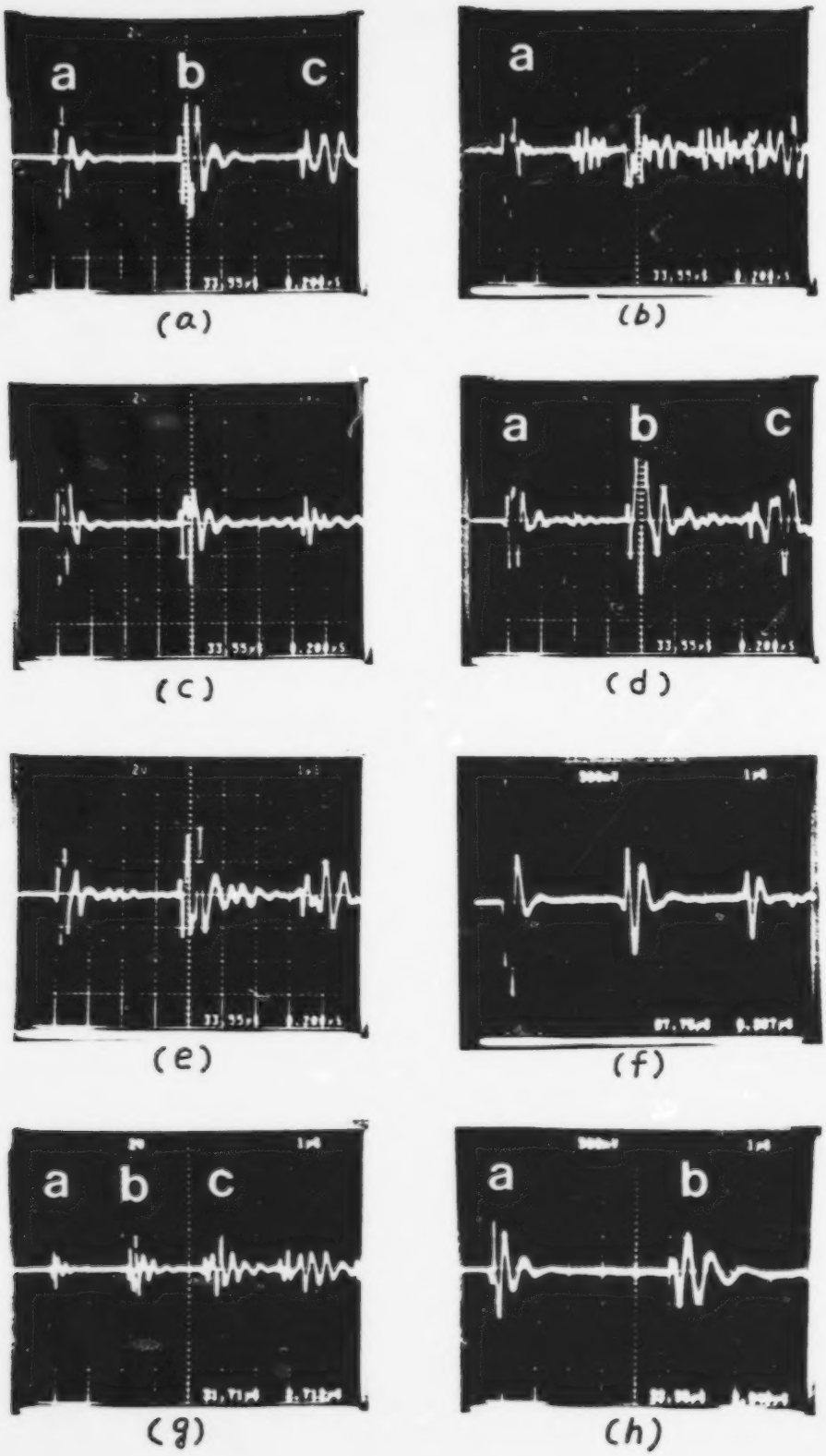

Fig.A4(a)-(h) The received echoes 'a', 'b' and 'c' for Al rods 'A', 'C', 'D', 'E', 'F', 'H', 'I' and 'J' using a pair transducers described in Fig.A2 in the transmission geometry respectivley. The amplitudes are arbitrary.

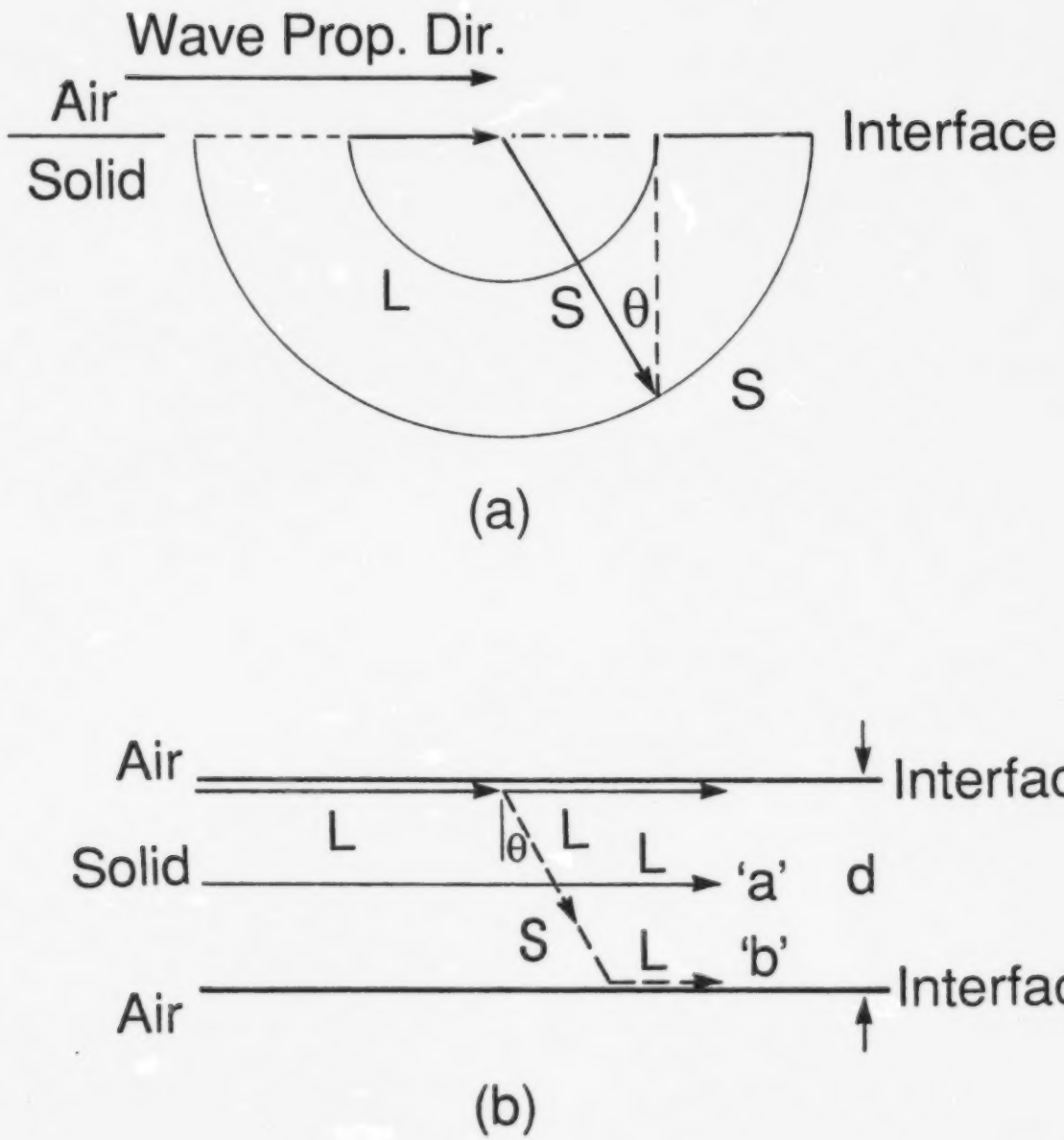

Fig.A5 (a) The phase matching requirements represented by the slowness curves for mode coversion processes which cause the trailing echoes, (b) the propagation paths for echoes 'a' and 'b'.

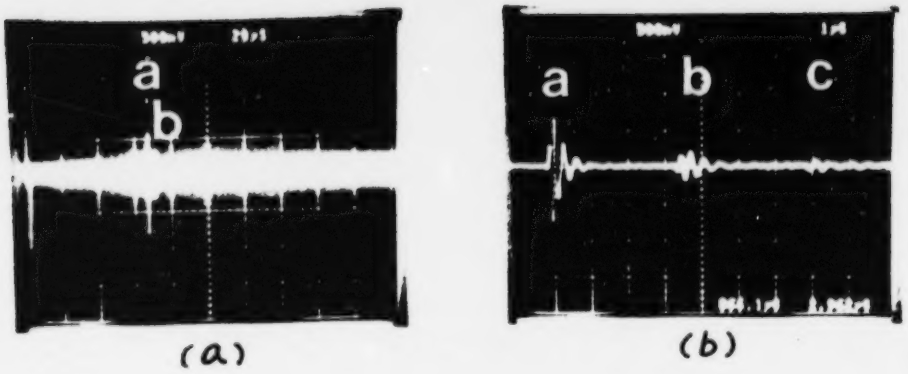

Fig.A6 (a) The reflected echoes through the Al Rod 'L' using a 5 MHz Ultran longitudinal transducer with a 12.7 mm diameter. (b) is the zoomed picture of (a).

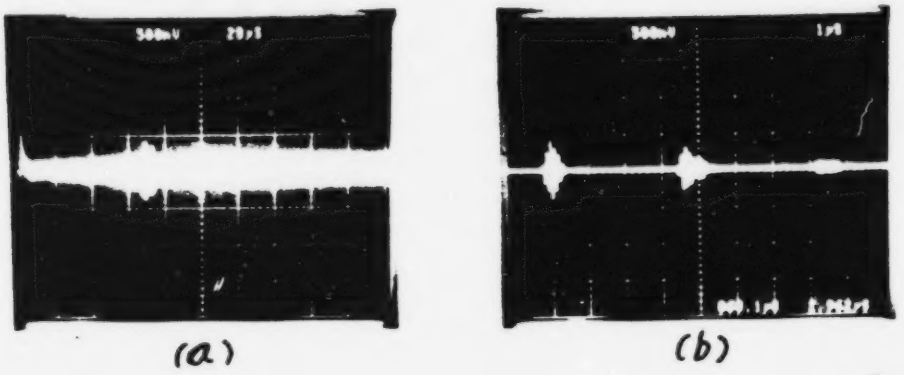

Fig.A7 (a) The received signals with a 25 MHz and 6.35 mm diameter KB-Aerotech longitudinal transducer and performed on the rod 'A'. (b) is the zoomed picture of (a).

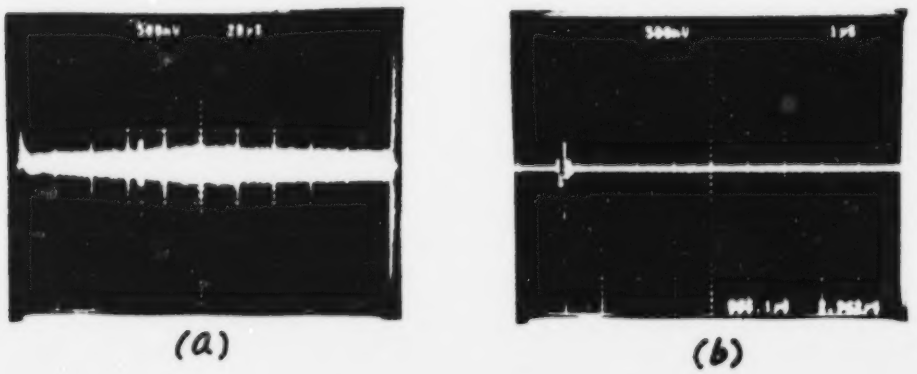

Fig.A8 (a) The received signals with a 25 MHz and 6.35 mm diameter KB-Aerotech longitudinal transducer and performed on the rod 'L'. (b) is the zoomed picture of (a).

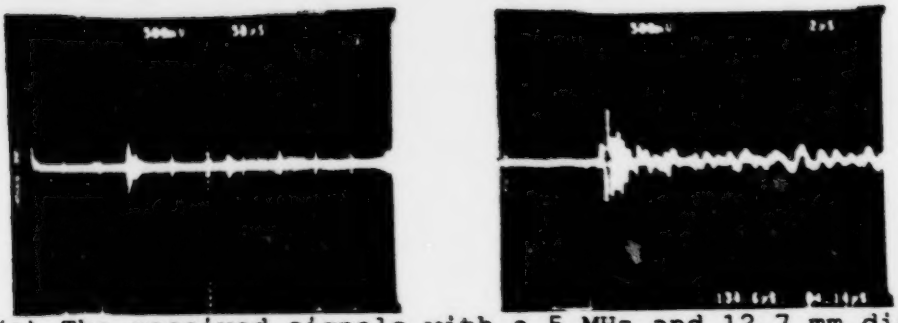

Fig.A9 (a) The received signals with a 5 MHz and 12.7 mm diameter Panametrics shear transducer and performed on the rod 'I'. (b) is the zoomed picture of (a).

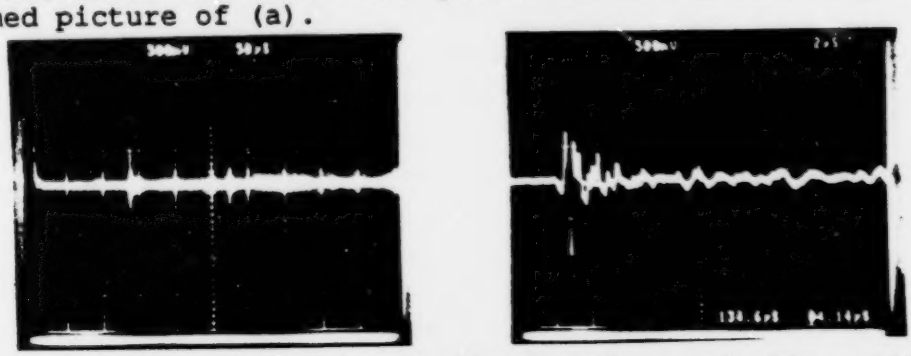

Fig.A10 (a) The received signals for the rod 'A' with the transducer described in Fig.A9. (b) is the zoomed picture of (a).

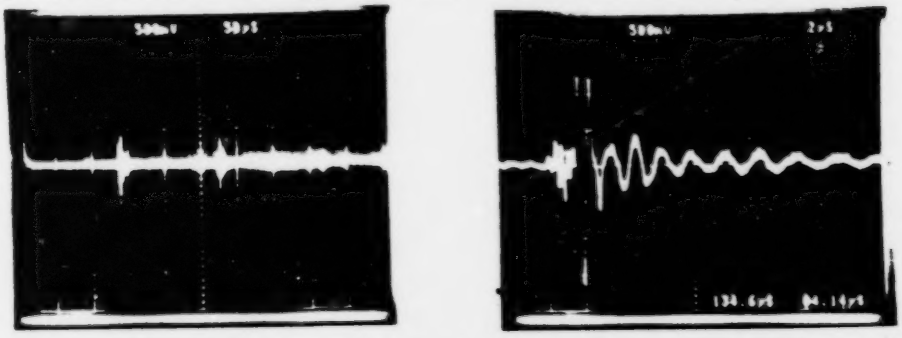

Fig.A11 (a) The received signals for the rod 'J' with the transducer described in Fig.A9. (b) is the zoomed picture of (a).

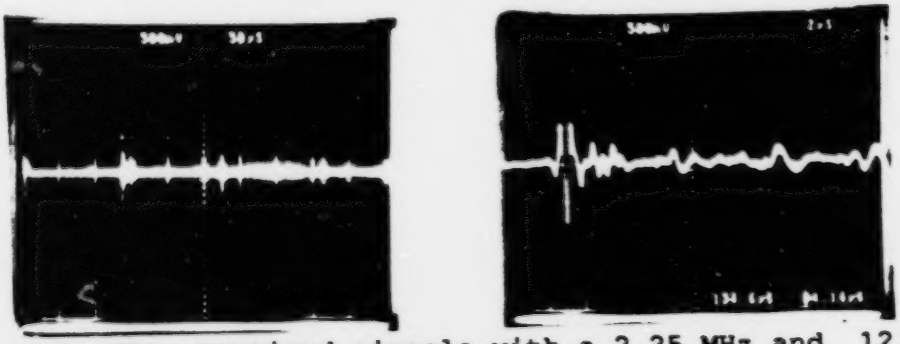

Fig.A12 (a) The received signals with a 2.25 MHz and 12.7 mm diameter Panametrics shear transducer and performed on the rod 'A'. (b) is the zoomed picture of (a).